J Neurophysiol 112: 1421–1438, 2014.
First published June 11, 2014; doi:10.1152/jn.00077.2014.

Temporal response properties of koniocellular (blue-on and blue-off) cells in marmoset lateral geniculate nucleus

A. N. J. Pietersen,[1,2] S. K. Cheong,[1,2] S. G. Solomon,[3,4] C. Tailby,[3,5] and P. R. Martin[1,2,3]

[1]*Australian Research Council Centre of Excellence for Integrative Brain Function, University of Sydney, Sydney, Australia;* [2]*Save Sight Institute, University of Sydney, Sydney, Australia;* [3]*School of Medical Sciences, University of Sydney, Sydney, Australia;* [4]*Department of Experimental Psychology, University College London, London, United Kingdom; and* [5]*Florey Institute of Neuroscience and Mental Health, Heidelberg, Australia*

Submitted 24 January 2014; accepted in final form 7 June 2014

Pietersen AN, Cheong SK, Solomon SG, Tailby C, Martin PR. Temporal response properties of koniocellular (blue-on and blue-off) cells in marmoset lateral geniculate nucleus. *J Neurophysiol* 112: 1421–1438, 2014. First published June 11, 2014; doi:10.1152/jn.00077.2014.— Visual perception requires integrating signals arriving at different times from parallel visual streams. For example, signals carried on the phasic-magnocellular (MC) pathway reach the cerebral cortex pathways some tens of milliseconds before signals traveling on the tonic-parvocellular (PC) pathway. Visual latencies of cells in the koniocellular (KC) pathway have not been specifically studied in simian primates. Here we compared MC and PC cells to "blue-on" (BON) and "blue-off" (BOF) KC cells; these cells carry visual signals originating in short-wavelength-sensitive (S) cones. We made extracellular recordings in the lateral geniculate nucleus (LGN) of anesthetized marmosets. We found that BON visual latencies are 10–20 ms longer than those of PC or MC cells. A small number of recorded BOF cells ($n = 7$) had latencies 10–20 ms longer than those of BON cells. Within all cell groups, latencies of foveal receptive fields ($<10°$ eccentricity) were longer (by 3–8 ms) than latencies of peripheral receptive fields ($>10°$). Latencies of yellow-off inputs to BON cells lagged the blue-on inputs by up to 30 ms, but no differences in visual latency were seen on comparing marmosets expressing dichromatic ("red-green color-blind") or trichromatic color vision phenotype. We conclude that S-cone signals leaving the LGN on KC pathways are delayed with respect to signals traveling on PC and MC pathways. Cortical circuits serving color vision must therefore integrate across delays in (red-green) chromatic signals carried by PC cells and (blue-yellow) signals carried by KC cells.

lateral geniculate nucleus; vision; color vision

THIS STUDY concerns response timing in subcortical visual pathways. The best-studied divisions of the subcortical visual system in primates are the parvocellular (PC) and magnocellular (MC) pathways. Compared with PC pathway cells, MC pathway cells show higher contrast sensitivity, especially at high temporal frequencies, and more rapid and phasic visual-evoked responses and have faster-conducting axons. For these reasons visual signals passing along the MC pathway are assumed to reach the cerebral cortices before the signals from PC pathways do (Bullier and Henry 1980; Lee et al. 2010; Lennie and Movshon 2005; Merigan and Maunsell 1993).

Less is known about response timing in the third division of the subcortical visual system, which comprises multiple ganglion cell types projecting through the koniocellular/interca-lated (KC) zones of the lateral geniculate nucleus (LGN). Geniculocortical projections of KC pathways include the supragranular layers of primary visual cortex (V1) as well as extrastriate cortical areas, but the way in which KC signals are integrated with PC and MC signals at subsequent levels of visual processing remains unclear (Casagrande and Xu 2003; Hendry and Reid 2000). The best-characterized KC cell type is the color-coding "blue-on/yellow-off" (BON) cell, which receives on-sign input originating in short-wave-sensitive (S or "blue") cone photoreceptors and off-sign input originating in medium (M)- and long (L)-wave-sensitive cone photoreceptors. A second, less frequently encountered "blue-off/yellow on" (BOF) cell shows a complementary pattern of cone inputs (Dacey and Lee 1994; Szmajda et al. 2006; Tailby et al. 2008b). The focus of the present study is on timing of these cells (BON and BOF) in comparison with timing of PC and MC pathway cells.

Direct measurements of S, L, and M cones showed that all cones had similar kinetics and sensitivity (Schnapf et al. 1990), and the S, M, and L cones have similar temporal characteristics where measured at the ganglion cell level (Yeh et al. 1995a). There is, however, broad agreement from psychophysical and physiological studies that S-cone signals in the brain are processed more slowly than medium and/or long (ML)-cone signals (Brindley et al. 1966; Lee et al. 2009; McKeefry et al. 2003; Smithson and Mollon 2004). More generally, there is a long-standing puzzle concerning the following discrepancy: human color vision shows a low-pass temporal frequency attenuation characteristic (de Lange 1958; Swanson et al. 1987), but responses of color-opponent ganglion cells and LGN cells in monkeys show band-pass temporal tuning with peak sensitivity near 10 Hz (Gouras and Zrenner 1979; Lee et al. 1990). This discrepancy might be partly explained if cortical circuits for color vision need to integrate across delays in (red-green) chromatic signals carried by PC cells and (blue-yellow) signals carried by KC cells.

Little difference in visual evoked response latency of PC, BON, and BOF cells was reported in central visual field of macaque monkeys (mean latencies of all groups were close to 60 ms; Tailby et al. 2008a), but a systematic study of a large cell sample has not been made. Furthermore, there is disagreement in the literature concerning the question of whether yellow-off responses are delayed relative to blue-on responses in BON cells; one in vitro study of macaque retina reported that the yellow-off response is delayed by ~18 ms relative to the blue-on response (Field et al. 2007), whereas other in vivo

Address for reprint requests and other correspondence: P. R. Martin, Sydney Eye Hospital Campus C09, 8 Macquarie St., Sydney 2001, Australia (e-mail: prmartin@physiol.usyd.edu.au).

studies and one in vitro study reported only negligible difference (Crook et al. 2009; Tailby et al. 2008b; Yeh et al. 1995a). Finally, understanding response latency in BOF cells may help clarify the retinal pathways underlying BOF signals. In macaque monkey fovea the S cones are reported to make off-sign connections to midget bipolar and ganglion cells (Klug et al. 2003). On the other hand, in ground squirrel retina the blue-off signals in ganglion cells arise via additional synapses (sign-inverting connections) of amacrine cells (Chen and Li 2012; Sher and DeVries 2012). If homologous sign-inverting circuitry is present in marmoset monkey retina, then the latency of BOF cells should be longer than the latency of BON cells.

Previous studies have analyzed responses to different kinds of stimuli (e.g., flashes, drifting gratings, pseudorandom checkerboards) to estimate visual response latencies. The question arises as to what extent differences between reported latencies can be attributed to different stimulus conditions. Here we addressed this question by comparing latency estimated for three different stimulus types and by measuring overlapping cell populations with different stimuli.

MATERIALS AND METHODS

Ethical approval. Procedures conformed to the Australian National Health and Medical Research Council (NHMRC) code of practice for the use and care of animals and were reviewed and approved by institutional animal care and ethics committees at the University of Sydney and University of Melbourne.

Animal preparation. Extracellular recordings were made from the LGN of 25 adult marmosets (*Callithrix jacchus*) obtained from the NHMRC combined breeding facility. Other data from cells in 19 of the animals were published previously (Cheong et al. 2011; Tailby et al. 2008b). Ten of the animals were female. The (dichromatic or trichromatic) color vision phenotype (Yeh et al. 1995b) of all but one of the female animals was determined by combination of genetic analysis (polymerase chain reaction-run length fragment polymorphism) and analysis of responses of PC pathway cells to cone-selective modulation as described previously (Martin et al. 2011). Six of the females showed trichromatic color vision phenotype with S receptor peak sensitivity near 423 nm and ML receptor peaks near 543 nm and 563 nm. One female and all male animals showed dichromatic color vision phenotype, with S receptor peak sensitivity near 423 nm and a single ML receptor type with peak sensitivity near 543 nm, 556 nm, or 563 nm.

Each animal was initially sedated with an intramuscular injection of 12 mg/kg Alfaxan (Jurox) and 3 mg/kg diazepam (Roche). Supplementary doses of Alfaxan were given as required during surgery. Subsequent surgery was performed under supplemental local anesthesia (lignocaine 2%; AstraZeneca). A tail vein was cannulized, the trachea exposed, and an endotracheal tube inserted. The head was placed in a stereotaxic frame, and a craniotomy was made over the right LGN. Anesthesia and analgesia were maintained by intravenous sufentanil citrate infusion (6–30 $\mu g \cdot kg^{-1} \cdot h^{-1}$; Sufenta Forte, Janssen Cilag, Beerse, Belgium) in physiological solution (sodium lactate, Baxter International) with added dexamethasone (0.4 kg/h; Mayne Pharma) and Synthamin 17 (amino acids 10%, 225 $mg \cdot kg^{-1} \cdot h^{-1}$; Baxter International). Muscular paralysis was induced and maintained by addition of pancuronium bromide (0.3 kg/h; AstraZeneca) to the infusion solution. The animal was artificially ventilated so as to keep the end-tidal CO_2 close to 3.7%. Electroencephalogram (EEG) and electrocardiogram signals were monitored. Dominance of low frequencies (1–5 Hz) in the EEG recording and stability of the EEG frequency spectrum under intermittent noxious stimulus (tail pinch) were taken as the chief signs of an adequate level of anesthesia. We found that low anesthetic dose rates in the range cited above were always very effective during the first 24 h of recording; thereafter, if drifts toward higher frequencies in the EEG record became evident, they were counteracted by increasing the rate and/or concentration of sufentanil administration through the tail vein cannula. The typical duration of a recording session was 48–72 h. Rectal temperature was kept near 37.5°C with a thermistor-controlled heating blanket. Additional antibiotics and anti-inflammatory drugs were given daily by intramuscular injection of 25 mg of penicillin (Norocillin, Norbrook) and 0.1 mg of dexamethasone. The pupils were dilated with atropine sulfate (dilated diameter 4–5 mm), and the corneas were protected with high-permeability contact lenses that remained in place for the duration of the experiment. Supplementary lenses (with power determined by maximizing the spatial resolution of the first receptive fields encountered for each eye) were used to focus the eyes at a distance of 114 cm.

A durotomy was made above the LGN, and a guide tube containing the recording electrode was inserted into the brain. Action potential waveforms of single cells were discriminated by principal component analysis of amplified voltage signals from single electrodes (5–11 MΩ; FHC, Bowdoin, ME) or tetrodes (2–5 MΩ; Thomas Recording, Giessen, Germany) with a recording surface separation of ~30 μm.

Visual stimuli. A front-silvered gimbaled mirror was used to bring the receptive field onto the center of a cathode ray tube (CRT) monitor (Sony G520; 100-Hz refresh rate). For each phosphor the relationship between the output of the video card and the photopic luminance was determined. The inverse of this relationship was applied to the signals that were sent to the video card. Visual stimuli were generated with a G5 Power Macintosh computer with custom software that also collected, discriminated, and time-stamped the recorded spike waveforms (EXPO/OpenGL; P. Lennie, University of Rochester, Rochester, NY). Stimuli were presented on a gray screen (guns set to half-maximum intensity) at mean luminance close to 50 cd/m^2 and mean chromaticity $x = 0.361$, $y = 0.363$. All stimuli were presented as excursions from this mean level. Allowing for the difference in posterior nodal distance between marmoset and human eye, the background level would correspond to ~1,500 Troland (Td). Visual stimuli were normally presented through the dominant eye only. Recorded spike time stamps were corrected post hoc for time delay due to the OpenGL frame buffer interface and CRT beam fly-time to the center of the screen. This delay was estimated to be ~25 ms by recording the "response" latency of a photodiode placed at the center of the screen. Stimuli were placed as close as practicable to the center of the screen in order to reduce latency variation due to the CRT beam fly-time.

A set of spectral absorbance templates (nomograms) with peak wavelengths corresponding to those present in a given animal was generated with a polynomial template (Lamb 1995). Lens absorbance was accounted for with published measurements for marmoset (Tovée et al. 1992). The contrast in a given class of cone generated by each stimulus was obtained by calculating the inner product of the relevant cone nomogram and the spectral power distribution of the (linearized) red, green, and blue guns specified by the stimulus. The resulting inner products (corresponding to cone activations elicited separately by the red, green, and blue guns) were then summed and expressed relative to their values at the white point (red, green, and blue guns set to the mean value), calculated in the same manner. The spectral power distribution of each gun was determined with a PR670 photometer (Photo Research, Palo Alto, CA). No correction was made for macular pigment because <10% of recorded fields (42 of 436) were located within 1° of the visual axis. Stimuli were designed to be achromatic, S cone isolating, or ML cone isolating. Variations in prereceptoral absorption can make the latter two stimuli deviate from the predicted cone-selective color direction. In previous work we demonstrated that bleed-through of signals from nominally silent cones is an important consideration in recordings from high-gain cells such as MC cells in the LGN (Tailby et al. 2008b). The nominal S cone-isolating stimulus produced 60–80% contrast in S cones and <5% contrast in ML cones. The nominal

ML cone-isolating stimulus produced >60% contract in ML cones and <2% contrast in S cones.

Previous studies have analyzed responses to different kinds of stimuli (e.g., flashes, drifting gratings, pseudorandom checkerboards) to estimate visual response latencies. The question arises as to whether differences between reported latencies can be attributed to the stimulus used. Here we compared latency estimated for three different stimulus types by measuring overlapping cell populations; we refer to these stimuli hereinafter as "Pulse," "Step," and "Check." In each case the stimulus field size was set to include the classical center and surround receptive field components.

The first stimulus type (Pulse stimulus) was designed to make estimates of latency with high (2 ms) accuracy, as close as possible to the instrumental limits set by the CRT display. A spatially uniform field was presented within a circular window typically between 1° and 2° in diameter. The Pulse stimulus comprised six contrast conditions (achromatic, ML cone-isolating, and S cone-isolating increments and decrements, presented as excursions from a mean gray background) plus one blank (zero contrast) condition. Each condition was presented 100 times for 200 ms with 300-ms interstimulus interval, yielding a total 50 s of data collected for each condition. Conditions were randomly interleaved. Stimuli were presented at 70% achromatic, ML cone, or S cone contrast. Example responses to the Pulse stimulus are shown in Fig. 1.

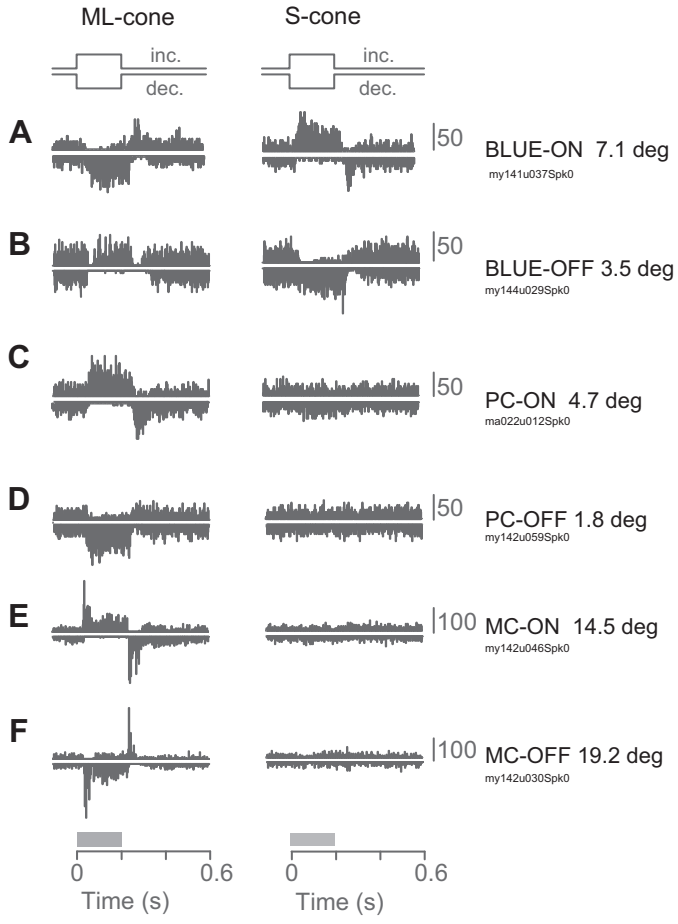

Fig. 1. Response profile. Example peristimulus time histogram (PSTH) responses to ML cone (*left*)- and S cone (*right*)-isolating Pulse stimuli. Each of *A–F* shows responses of a single cell with receptive field classification and distance from the fovea indicated. For each cell increments and decrements are paired, with the decrement response shown inverted. Stimulus duration is indicated by the gray bar on the time axis. PC, parvocellular; MC, magnocellular.

The second stimulus type (Step stimulus) has been used in our laboratories for over 10 years as part of a standard test battery for cell classification and supplies a large database of cells (including the rarely encountered BOF cells) for analysis. Step stimulus responses are collected over a smaller number of trials than is the case for the Pulse stimulus, and the bin resolution (5 ms) is lower than that for the Pulse stimulus (2 ms). The stimulus comprised a uniform field presented within a circular window typically between 2° and 4° in diameter; 51% of cells were measured with a window of 2° or less. These window sizes will encompass the center and surround components of the classical receptive field. The temporal profile was square-wave modulation at 0.5 Hz for 4 s (i.e., 2 stimulus cycles) with the screen held at background luminance for 0.5 s between presentations. The adaptation take-off point is thus different for the first and second cycles of the stimulus. Randomly interleaved achromatic, S cone-isolating, and ML cone-isolating conditions were presented for a total 8–20 s of data collection for each condition. The achromatic stimulus was normally presented at 90% contrast; the S cone-isolating and ML cone-isolating stimuli were presented at 80% cone contrast.

The third stimulus type (Check stimulus) was designed to test whether discrepancies in the literature regarding temporal characteristics of MC, PC, and KC cells can be attributed to stimulus conditions rather than true differences between the pathways. For example, studies using large-field temporal modulation found that on-center and off-center cells show symmetric temporal properties (Kremers et al. 1993; Lankheet et al. 1998), whereas a study using white noise stimulation reported more rapid response kinetics in on-center than off-center cells (Chichilnisky and Kalmar 2002). The Check stimulus comprised a pseudorandom white noise checkerboard (16 × 16-element square field). The field size was adjusted to encompass the classical receptive field(s) at the recording site. For achromatic stimulation, the luminance of each Check element was drawn from a Gaussian distribution centered on the mean luminance. A parallel method was used for S cone-isolating checkerboards; here the [R G B] values of each element were specified with the spectral convolution procedure outlined above. The standard deviation of the Gaussian distribution was 0.3, where +1 is the maximum achievable luminance or S-cone contrast increment. The element values were updated every 30 ms.

In addition to the stimuli described above, we measured (for most recorded cells) responses to drifting (5 Hz) sine gratings of variable spatial frequency and contrast in order to characterize the receptive field dimensions and contrast sensitivity. Grating responses of most of the cells in the present study were reported previously (Cheong et al. 2013; Tailby et al. 2008b); all responses were reanalyzed for the present purpose.

Cell classification. PC, MC, BON, and BOF cells were distinguished by receptive field properties (Cheong et al. 2013; Dreher et al. 1976; Kaplan and Shapley 1986; Wiesel and Hubel 1966). Most of the electrode tracks through the LGN were also anatomically reconstructed as described previously (Szmajda et al. 2006; White et al. 2001). For all cells the sign (on-center or off-center) and contrast response function were determined. BON cells are distinguished by their vigorous excitatory response to an S cone-isolating stimulus (Dacey and Lee 1994; Derrington et al. 1984; Tailby et al. 2008a; Yeh et al. 1995b). PC cells show sustained response to maintained contrast and linear contrast-response function. MC cells show transient responses to maintained contrast, saturating contrast response function, and response phase advance from intermediate to high contrast levels (Kaplan and Benardete 2001; Lee et al. 1994; Martin and Solomon 2013; Solomon et al. 2002a). Latencies were calculated from responses to each cell's preferred contrast sign.

The depth below cortical surface of each cell was recorded from the hydraulic microelectrode advance (David Kopf model 640). At conclusion of single-cell recordings, the animal was given an intravenous overdose of 120 mg/kg pentobarbital sodium (Lethabarb, Virbac) and then transcardially perfused with 0.9% saline followed by 4% para-

formaldehyde. We confirmed the anatomical location of 55% (61/111) of the cells presented with the Pulse stimulus. In cases where track location was not determined, we used the receptive field properties, eye dominance, and encounter position together with the functional differences outlined above to classify the cells. On this basis, from 15 recorded BON cells we classified 6 (40%) to layer K3 (between internal PC and internal MC layers), 4 (27%) to layer K4 (between internal and external PC layers), and 1 to layer K2 (between internal and external MC layers). From 7 recorded BOF cells we located 4 (57%) to layer K3, 1 to layer K2, and 1 to the internal PC layer. The locations of 4 BON cells and 1 BOF cell could not be assigned with confidence.

Data analysis. For analysis of responses to Pulse and Step stimuli, the action potential times were folded into a peristimulus time histogram (PSTH). The Pulse stimulus was analyzed with a bin width of 2 ms; the Step stimulus was analyzed with a bin width of 5 ms. The first two consecutive bins in the PSTH where response rate was two or more standard deviations above the mean maintained discharge rate (measured in a separate "blank" trial) were determined. A linear regression was calculated from the first of these bins to the bin containing the initial response peak. This line was back-extrapolated to the maintained discharge rate, and the time of the intersection was taken as response onset latency. The onset-to-peak time is the time between onset latency and the response peak located from a five-point moving average. Mean response profiles for grouped data were calculated using each cell's PSTH normalized to the peak of a five-point moving average. For some cells response latency was also estimated from linear regression of response phase for low-spatial-frequency (<0.01 cyc/°) drifting gratings presented at temporal frequencies between 1 Hz and 40 Hz. Latency is referred to the zero crossing for preferred contrast sign.

We characterized the response time course for the Pulse and Step stimuli as follows. The average response amplitude during the final 100 ms of the stimulus presentation was defined as the sustained part of the response. A transience index was calculated as the peak response amplitude minus the sustained part of the response, divided by the peak response amplitude. The maintained discharge rate was first subtracted from both the peak and sustained part of the response for this calculation.

We characterized the sensitivity of cells to the monitor refresh rate ("frame-locking") as follows. The 75 ms to 175 ms segment of the response to the Pulse stimulus was analyzed with fast Fourier transform, and the resulting frequency spectrum was normalized to the value of the zero-order Fourier component (Szmajda et al. 2006; White et al. 2001). The amplitude of the bin at 100 Hz was taken as the frame-locking index.

At a refresh rate of 100 Hz the CRT beam reaches the center of the screen ~5 ms after the beginning of the frame draw cycle. To test whether our recording precision is high enough to detect this delay, we recorded responses of one MC cell to the Pulse stimulus at each of three locations on the CRT screen, by successively moving the receptive field position via the gimbaled mirror referred to above. The latency measured at the top left of the screen (11.8 ms) was almost 10 ms shorter than the latency measured at the bottom right of the screen (21.5 ms). The latency measured near the center of the screen was 17.5 ms. Since >85% of our measurements were made within 5 cm (vertical) of the screen center we thus can estimate the measurement precision to be better than 2 ms.

Check analysis. We calculated the spike-triggered average for each element in the Check stimulus by reverse correlation (Chichilnisky 2001; Solomon et al. 2010). The response temporal kernel was taken as the spike-triggered average time course of the Check element that generated the greatest spike-triggered average temporal variance. The time to the first peak (on-center cells) or trough (off-center cells) was taken as a measure of latency. The reader should note that these values are expected to be longer than the (escape from baseline) onset values calculated for responses to the Pulse and Step stimuli. To create a normalized temporal profile of the kernel data, the response from off-center cells was reversed in sign and all temporal kernels were normalized to the peak of their response. Average temporal kernels were calculated from the normalized data.

Grating responses. Receptive field dimensions were quantified by fitting the spatial frequency tuning curve with a difference-of-Gaussian (DOG) model (Croner and Kaplan 1995; Enroth-Cugell and Robson 1966):

$$R = C\left[\left(K_c \pi r_c^2 e^{-(\pi r_c f)^2}\right) - \left(K_s \pi r_s^2 e^{-(\pi r_s f)^2}\right)\right]$$

where R is response amplitude (imp/s), C is Michelson contrast of the stimulus, and f is the spatial frequency of the stimulus (cyc/°). The free parameters (K_c, center sensitivity; r_c, center radius; K_s, surround sensitivity; r_s, surround radius) were optimized with the *nlsqfit* function in MATLAB (MathWorks, Natick, MA).

Statistics. Data are presented as means ± SE unless stated otherwise. Multiple group comparisons were made with Kruskal-Wallis nonparametric analysis of variance (criterion P value 0.02) with post hoc Bonferroni-corrected multiple pairwise comparison (MATLAB functions *kruskalwallis* and *multcompare*, criterion P value 0.05). Two-group comparisons were made with the Wilcoxon nonparametric rank sum test with criterion P value 0.02.

RESULTS

The data presented in this article are based on responses of 444 LGN cells (232 PC, 159 MC, 46 BON, 7 BOF). Not all tests were run on all cells. In the following, we first show that MC cells have the shortest latency, followed by PC cells and then BON and BOF cells. Second, we show that there is negligible difference in onset latency between on-center and off-center cells within the MC and PC groups. In contrast, the BON and BOF populations show temporal asymmetry in which BOF responses lag BON responses by 10–20 ms. Third, we show that onset latencies of all cell groups are shorter in peripheral than in central visual field, but no differences in response latency were seen on comparing cells recorded in dichromatic or trichromatic marmosets. Fourth, we show that the ML-off latency is longer than the S-on latency in BON cells. Finally, we show that MC cell responses are more susceptible to video frame rate entrainment ("frame-locking") than PC or BON responses.

Response characteristics: examples. Figure 1 shows example PSTH responses to the Pulse stimulus. Each row shows responses of a single cell. Figure 1, *left*, shows responses to ML cone-isolating pulses, and Fig. 1, *right*, shows responses to S cone-isolating pulses; the receptive field classification and distance from the fovea are shown on the right. To facilitate comparison, the PSTHs for increments and decrements are paired, with the decrement response shown inverted. The blue-on cell (Fig. 1*A*) shows vigorous excitatory response to S cone increment and ML cone decrement, with transient excitatory "rebound" responses at offset of nonpreferred contrast polarity (i.e., ML cone increment, S cone decrement). The ML-off response shows a more sluggish onset than the S-on response (we return to this difference below). The blue-off cell (Fig. 1*B*) shows weak excitatory response to S cone decrement and ML cone increment. This blue-off cell also shows a partial "suppressed-by-contrast" characteristic (evidenced by transient inhibition at response onset and offset for ML cone increments) as previously reported (Solomon et al. 2010). Response onset for S cone decrements is sluggish.

Responses of PC and MC pathway cells to pulsed increments and decrements conform nicely to expectations from the

literature (e.g., Kremers et al. 1993). PC cells (Fig. 1, *C* and *D*) show sustained responses to preferred-polarity ML cone pulse, and MC cells (Fig. 1, *E* and *F*) show transient responses. The on-center and off-center pairs of PC and MC cells show almost exact mirror-symmetric responses, with the exception that the rebound response to offset of nonpreferred stimuli is more marked in on-center than in off-center cells. As expected (Sun et al. 2006; Tailby et al. 2008b), PC and MC cells show little or no response to S cone increment or decrement pulses. Lack of response indicates no functional input from S cones to the PC and MC cells, and also confirms the accuracy of our cone-isolating stimuli. In summary, these example responses indicate that in addition to the established differences in cone inputs, the blue-on and blue-off populations show temporal asymmetry in responses to temporal contrast, across both cell class (on vs. off) and cone inputs (S vs. ML). In the following sections we quantify these differences and show that they hold across cell populations at different eccentricities, under different stimulus conditions, and across dichromatic and trichromatic color vision phenotypes in marmosets.

Response latency measurement. Figure 2 illustrates onset latency measurements for three typical cells. Figure 2*A* shows PSTHs calculated by averaging responses across 100 stimulus presentations. For PC and MC cells an achromatic pulse was used; for the BON cell an S cone-isolating increment pulse was used. The black bar below each PSTH indicates stimulus duration. Figure 2*B* shows the responses to the first 75 ms of the stimulus on an expanded timescale. The MC cell (Fig. 2, *bottom*) has the shortest onset latency (16 ms), steepest onset slope, and most transient response profile of these examples. The PC cell (Fig. 2, *middle*) onset latency is longer (21 ms), and the BON cell (Fig. 2, *top*) has the longest onset latency (32 ms). Spatial

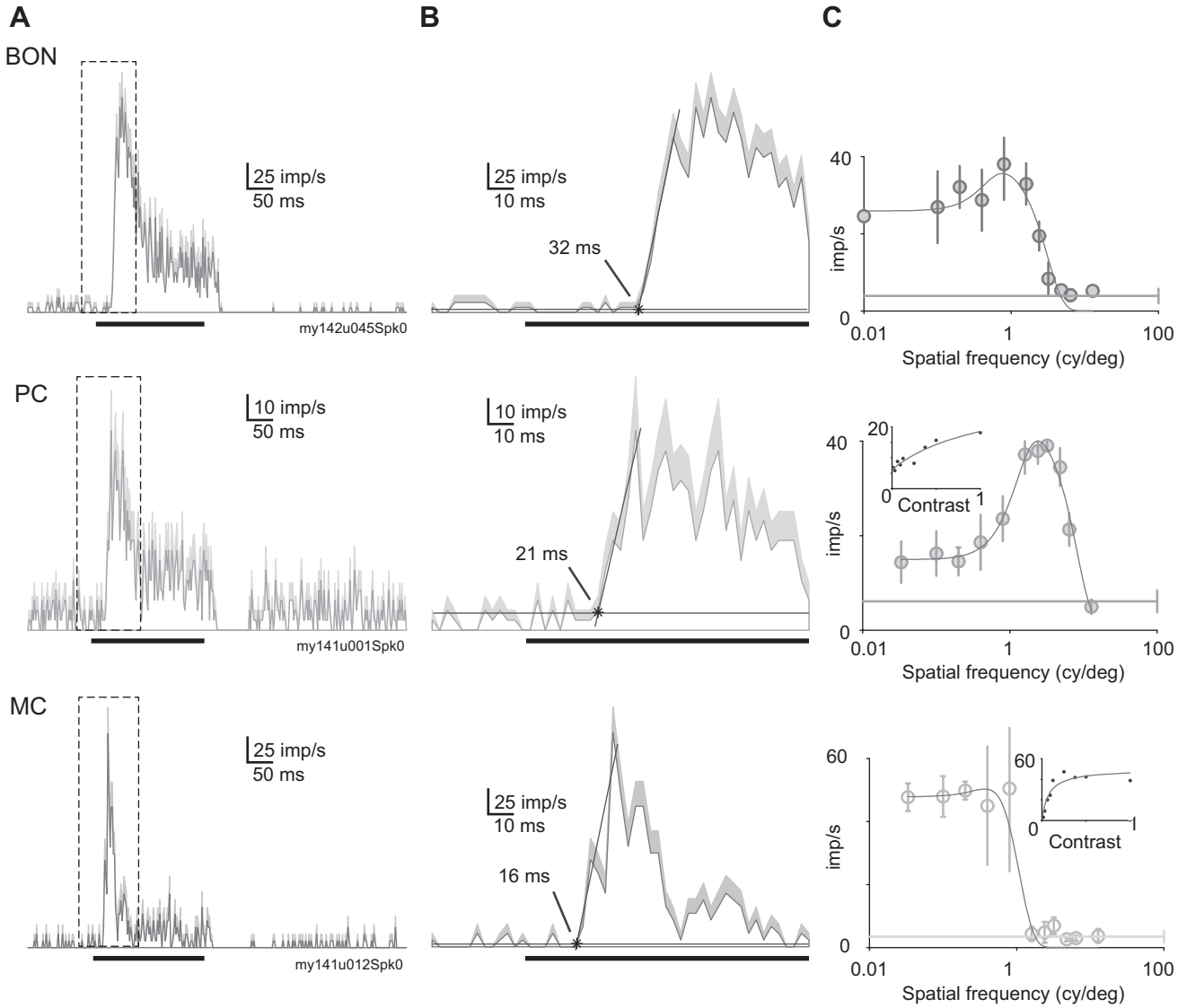

Fig. 2. Example responses. Representative examples of a PC, a MC, and a blue-on (BON) cell to the Pulse stimulus. *A*: representative example PSTHs. Horizontal bar below each PSTH indicates stimulus duration. PSTHs are made from 100 stimulus presentations. *B*: enlargement of the first 75 ms after stimulus onset. Shaded region above each PSTH shows the response SE. Star indicates onset latency. *C*: spatial frequency tuning curves for drifting high-contrast sine gratings show the expected properties for these cell classes: the BON cell shows high-amplitude and mild band-pass tuning for S cone-selective gratings; PC cells show strong band-pass tuning and respond to high spatial frequencies; MC cells show poor response to high spatial frequencies and saturated responses to lower frequencies. *Inset* graphs for PC and MC cells show contrast-response functions for low spatial frequencies. Note high-gain, saturating response in MC cell. Error bars show SDs. Solid lines show maintained response rate. Curves show difference-of-Gaussian fits for spatial frequency as described in the text.

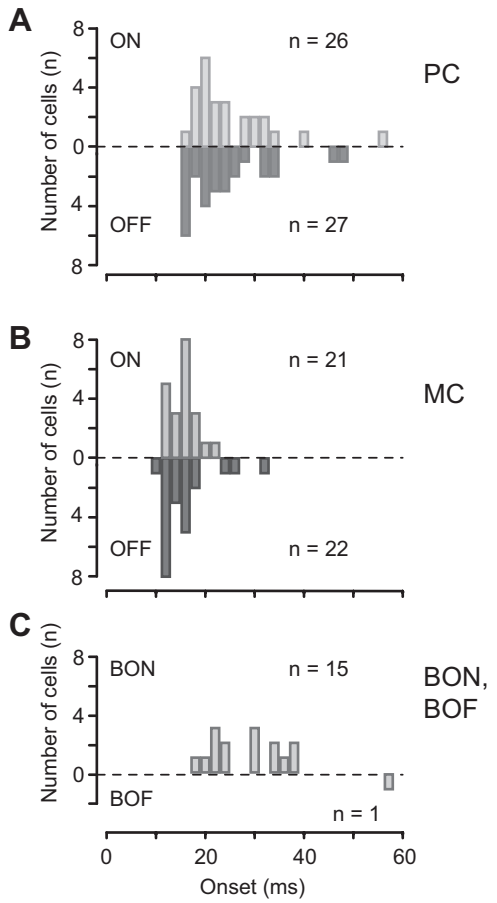

Fig. 3. Comparison of on-center and off-center cell latency, Pulse stimulus. *A*: onset latency of PC cells. Cells responding to the ON stimulus phase shown upwards (light bars) and cells responding to the OFF stimulus phase shown downwards (dark bars). *B*: MC cells. Note the similar latency distribution of on-center and off-center cells in PC and MC populations. *C*: BON and blue-off (BOF) cells.

frequency and contrast tuning curves for these cells are shown in Fig. 2*C* as an indication of how the PC, MC, and BON populations were distinguished in our experiments. In the next section, we compare response latency in on-center and off-center populations; in a later section we analyze the response time course in more detail.

Comparison of on-center and off-center cells. On- and off-responses are formed at the cone-to-bipolar cell synapse in the retina, by selective expression of metabotropic glutamate receptors in on-center bipolar cells and expression of ionotropic [α-amino-3-hydroxy-5-methyl-4-isoxazole-propionic acid (AMPA) and/or kainate] receptors in off-center bipolar cells (Haverkamp et al. 2001; Vardi et al. 2000). Although fed by these distinct synaptic mechanisms, on- and off-center ganglion cells show largely symmetric patterns of response timing in in vivo recordings (Lankheet et al. 1998; Martin et al. 2011; Yeh et al. 1995a). Subtle asymmetries (response dynamics of on-center cells are brisker and more linear than those of off-center cells) were, however, reported in in vitro recordings (Chichilnisky and Kalmar 2002). We therefore compared response latency in on- and off-center cells. Figure 3, *A* and *B*, show latency of on-center and off-center cells within the PC (Fig. 3*A*) and MC (Fig. 3*B*) groups. There is negligible difference between PC on-center (26.4 ± 1.7 ms, $n = 26$) and PC off-center (25.2 ± 1.7 ms, $n = 27$, $P = 0.55$) cells or between MC on-center (16.6 ± 0.6 ms, $n = 21$) and MC off-center (16.7 ± 1.2 ms, $n = 22$, $P = 0.25$) cells. Latency estimates were taken from response to Pulse stimulus; parallel analyses of responses to Step and Check stimuli likewise showed negligible differences between on-center and off-center cells (Step: PC, $P = 0.59$; MC, $P = 0.07$; Check: PC, $P = 0.07$; MC, $P = 0.27$). Figure 3*C* shows the onset latency data for BON cell responses (29.2 ± 1.8 ms, $n = 15$). Onset latency for one BOF recorded with the Pulse stimulus was 58 ms. For a larger sample of BOF cells recorded with the Step stimulus the latency (46.7 ± 4.5 ms, $n = 6$) was ~5 ms longer than that of BON cells recorded with the Step stimulus (42.2 ± 3.5, $n = 36$, $P = 0.13$). These results are tabulated in Table 1. In summary, we did not find significant difference between on-center and off-center cells across PC and MC layers but found that BOF responses lag BON responses by 5–30 ms.

Effect of receptive field eccentricity and center size on onset latency. In this section we investigate how onset latency depends on distance of the receptive field from the fovea (eccentricity). Figure 4*A* shows onset latencies for the Pulse stimulus. There is a significant negative correlation between onset latency and eccentricity when all groups are considered together (correlation coefficient: −0.45, $r^2 = 0.2$, $P < 0.02$, $n = 111$). Within groups, PC and BON cells show negative correlation (PC: correlation coefficient −0.42, $P < 0.02$; BON: correlation coefficient −0.61, $P < 0.02$). The MC cells show weak negative correlation that is not significantly different from zero (−0.23, $P = 0.14$), but there are few recordings from MC cells in the central 5°.

For all cell classes described in primates, the receptive field center size increases with eccentricity. Furthermore, responses

Table 1. *Onset latencies comparing preferred response sign*

Stimulus	Cell Type	ON	OFF
Pulse	MC	16.6 ± 0.6 ($n = 21$)	16.7 ± 1.2 ($n = 22$)
	PC	26.4 ± 1.7 ($n = 26$)	25.2 ± 1.7 ($n = 27$)
	BON	29.2 ± 1.8 ($n = 15$)	58 ($n = 1$)
Step	MC	24.9 ± 2.6 ($n = 26$)	32.5 ± 3.2 ($n = 36$)
	PC	37.0 ± 1.6 ($n = 91$)	34.8 ± 1.2 ($n = 90$)
	BON, BOF	42.2 ± 3.5 ($n = 36$)	46.7 ± 4.5 ($n = 6$)
Check	MC	19.8 ± 0.7 ($n = 55$)	21.2 ± 1.1 ($n = 41$)
	PC	34.9 ± 0.9 ($n = 42$)	32.6 ± 0.9 ($n = 32$)
	BON	33.6 ± 1.6 ($n = 11$)	

Data are presented as mean ± SE (group size in parentheses) onset latency to the stimuli used in this study for 3 different cell types split by preferred sign (on-center and off-center). MC, magnocellular; PC, parvocellular; BON, blue-on; BOF, blue-off.

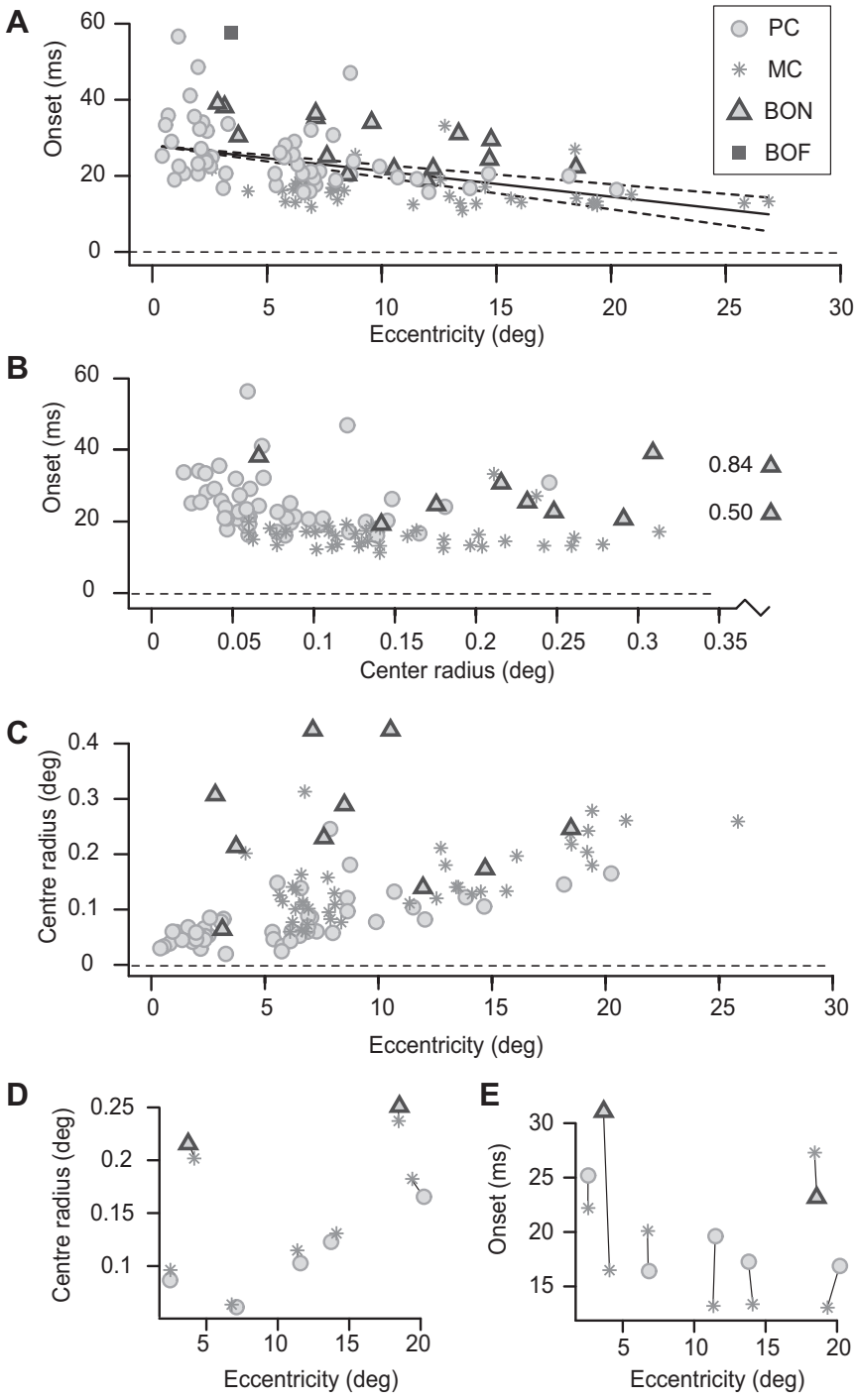

Fig. 4. Eccentricity dependence of onset latency. *A*: scatterplot of onset latency for the Pulse stimulus against receptive field eccentricity (distance from fovea) for each cell. Solid dark line shows linear regression of all cells (correlation coefficient = −0.45, $r^2 = 0.2$, $P < 0.02$, $n = 111$). Dashed lines show 95% confidence intervals. *B*: onset latency against receptive field center radius recovered from difference-of-Gaussian fit to drifting gratings. *C*: center radius as a function of eccentricity. *D*: 7 example cell pairs with closely matched eccentricity selected from the data shown in *C*. Members of each pair are joined by a straight line. *E*: onset latency of the eccentricity-matched pairs shows that the majority of MC cells have more rapid onset than their PC counterparts.

of all ganglion cell classes are more transient in peripheral than in central retina (Kaplan and Benardete 2001; Solomon et al. 2002a, 2005), indicating a link between receptive field spatial and temporal properties. We therefore asked whether response onset latency depends on receptive field center size. The result (for those cells where both measurements were made) is shown in Fig. 4*B*. Here it is apparent that over a wide range of center radius (0.05° to at least 0.3°) the MC and BON populations form parallel horizontal clouds, with BON cells consistently ~20 ms slower than MC cells at all center sizes. Over this center size range most PC receptive fields show intermediate latency values. These data show for BON and MC cells that onset latency is not strongly dependent on receptive field size. The smallest PC fields tend to show longer latencies than the largest PC fields. However, as expected (Fig. 4*C*), the smallest PC fields are close to the fovea, making the effects of eccentricity per se hard to disentangle from effect of receptive field size for PC cells. We attempted to address the question of whether there are intrinsic latency differences between PC, MC, and BON cells by picking from the data shown in Fig. 4*C* a set of cell pairs with closely matched center radius. This was possible for 10 cell pairs recorded between 4° and 20° eccentricity (8 MC+PC pairs, 2 MC+BON pairs; examples shown in Fig. 4*D*). Six of the eight MC cells showed more rapid onset latency than their PC cell counterparts (examples shown in

Fig. 4*E*); this difference was, however, not significant ($P > 0.05$, χ^2-test, Yates correction applied). The two MC+BON pairs tested showed no consistent difference (Fig. 4*E*). In sum, we found no obvious differences between the MC, PC, and BON classes when cell pairs were equated both for receptive field diameter and eccentricity, but the sample of cells meeting these criteria is too small to draw a firm conclusion. For simplicity in further analyses we divided our data into two groups, with distance from the fovea below or above 10°; we refer to these as the central and peripheral populations.

Response time course: pulse stimulus. Figure 5 shows example raster plots and average normalized PSTHs of responses to the Pulse stimulus. The raster plots above each PSTH are taken from three representative cells in each population. Overt frame-locking is readily visible (as vertical lines in the raster plots and by the "comb" appearance of the average PSTH) in the peripheral MC cell sample (Fig. 5*B*); we treat frame-locking in more detail in a later section of the present study.

Overall the PC, MC, and BON cell populations showed significant differences in transience ($P < 0.02$) and onset-to-

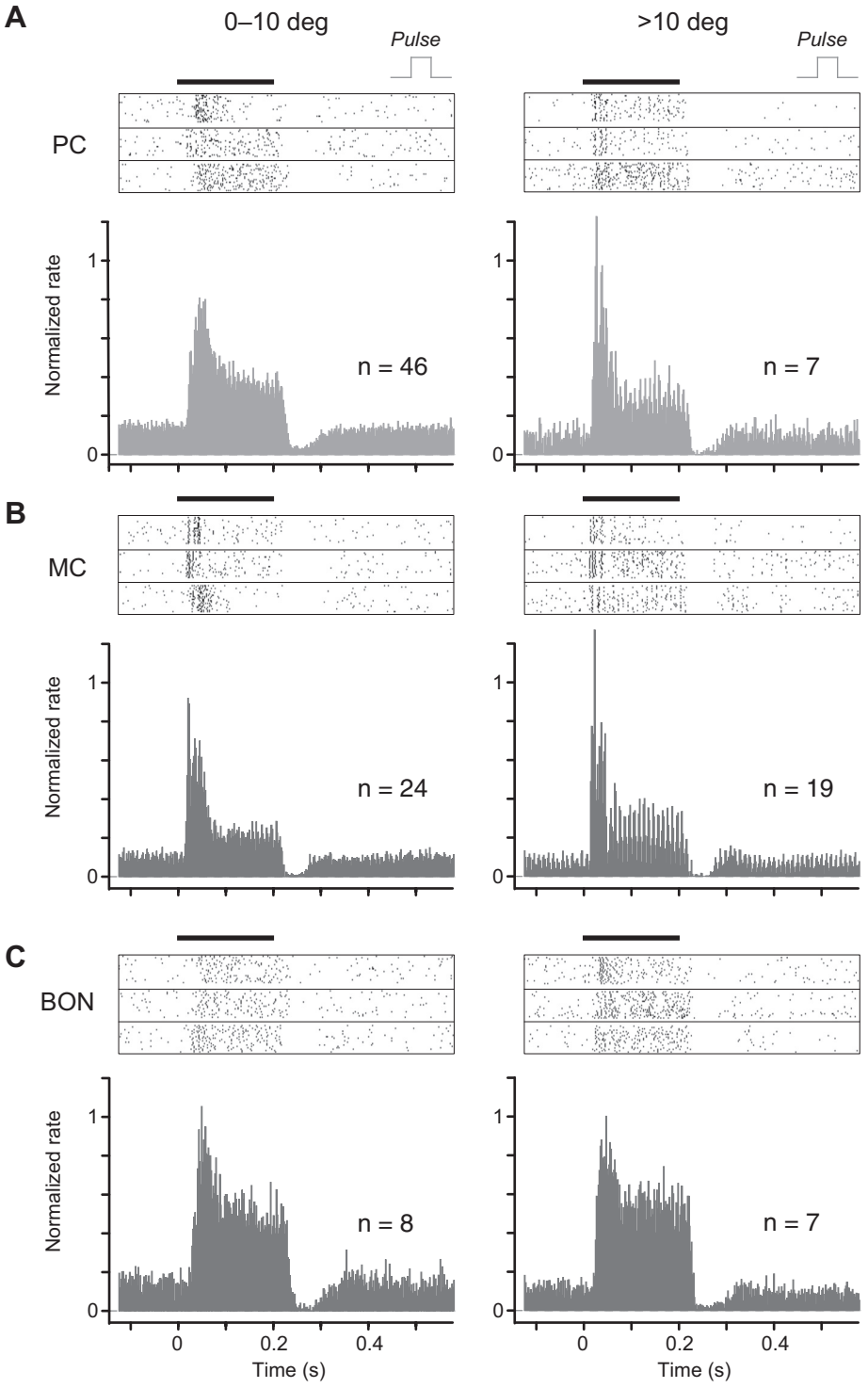

Fig. 5. Response time course, Pulse stimulus. Examples and normalized average responses to the Pulse stimulus. *A*: PC cell responses to achromatic 200-ms pulse at 70% contrast. Raster plots show 3 examples illustrating variety of response time course. Black horizontal bar indicates stimulus duration. PSTH shows normalized average response time course, calculated as described in the text. *Left*: receptive field eccentricities below 10°. *Right*: eccentricities above 10°. *B*: MC cell responses, achromatic pulse. Note overt frame-locking for average histogram above 10° eccentricity, visible as "comb" pattern on the PSTH. *C*: BON cell responses, S cone-isolating pulse, 80% cone contrast. Note absence of frame-locking.

peak times ($P < 0.02$). These differences cannot be attributed simply to variation in response magnitude between the tested classes. The most effective stimulus produced vigorous responses with comparable amplitude in all cell classes (Fig. 1, *A* and *C–F*), with the exception of some of the BOF receptive fields (e.g., Fig. 1*B*). The MC responses are the most transient. The transience index (where higher values represent more transient responses; see MATERIALS AND METHODS) of MC cells (0.86 ± 0.02, $n = 43$) is higher than that of PC cells (0.74 ± 0.2, $n = 52$, $P < 0.02$) and BON cells (0.54 ± 0.05, $n = 15$, $P < 0.02$). Furthermore, PC cells are more transient than BON cells ($P < 0.02$). It is also apparent (and expected: Solomon et al. 1999, 2002a) that responses in each cell class are more transient in peripheral compared with central retina. These trends were, however, only significant ($P < 0.02$) for MC cells. The reader should note that frame-locking will tend to reduce transience measures (because the baseline firing is increased on each frame); thus the temporal response differences between MC, PC, and BON classes may be underestimated by the statistics given above (Kaplan and Benardete 2001; Kremers et al. 1993; Solomon et al. 2002a). These results add to the established relationship (that is, PC cell responses are more sustained than MC cell responses) by showing that BON cell responses (and likely BOF cell responses) are more sustained than those of PC or MC cells.

MC cells show shortest onset-to-peak time (10.9 ± 1.2 ms, $n = 43$), indicating the most brisk response onset time course. This value is shorter than that of PC cells (17.1 ± 1.3 ms, $n = 53$, $P < 0.02$) but not BON cells (15.8 ± 2.2 ms, $n = 15$, $P > 0.02$); there is also little difference between PC and BON cells ($P > 0.02$). On comparing central and peripheral populations there is no significant difference in onset-to-peak time for PC and BON cells ($P > 0.2$), but the onset-to-peak time for central MC cells (13.8 ± 1.7 ms, $n = 24$) is greater than that of peripheral MC cells (7.2 ± 1.1 ms, $n = 19$; $P < 0.02$). The response of the single BOF cell measured with the Pulse stimulus was very sluggish (Fig. 1*B*), showing slow increase over the 200 ms of stimulus presentation. Overall these data imply that a brisk onset time course is associated with more transient (i.e., MC) cell responses.

Response time course: Step and Check stimuli. We next consider responses to the Step and Check stimuli. For Pulse stimuli the intensity increments (for on-center cells) and decrements (for off-center cells) depart from the same adaptation level (i.e., the background screen luminance), but for the Step stimulus the take-off adaptation level is higher for the decrement than for the increment. As explained in MATERIALS AND METHODS, this shortcoming in the stimulus is offset by the fact that our database of responses to the Step stimulus is large ($n > 30$ for all groups except BOF), allowing responses across cell class and visual field eccentricity to be compared. Figure 6*A* shows normalized average PSTHs of responses to the Step stimulus for BON cells (Fig. 6*A*, *top*), PC cells (Fig. 6*A*, *middle*), and MC cells (Fig. 6*A*, *bottom*). The pattern is similar to that seen for the Pulse stimulus (for overall group differences, $P < 0.02$): MC cell responses are most transient (transience index 0.73 ± 0.02, $n = 62$), followed by PC cells (0.69 ± 0.1, $n = 181$; Fig. 6*A*) and BON cells (0.58 ± 0.03, $n = 36$). No significant differences in transience or onset-to-peak time were seen on comparing central and peripheral cells within each cell type (data not shown). We conclude that the broad differences between PC, MC, and BON cells outlined above for the Pulse stimulus are applicable to the larger population measured (albeit at lower temporal precision) with the Step stimulus.

Figure 6*B* shows the normalized average temporal kernels and standard deviations for the Check stimulus, arranged by cell type and eccentricity group. The spike-triggered average response is extracted from the checkerboard pixel showing greatest response variance; this pixel was always close to the center of the excitatory ("center") receptive field region. For the Check stimulus we characterized response transience by the full width at half-maximum height (FWHH) of the temporal kernel, as shown in Fig. 6*B*. In agreement with the pattern set by responses to the Pulse and Step stimuli, the PC, MC, and

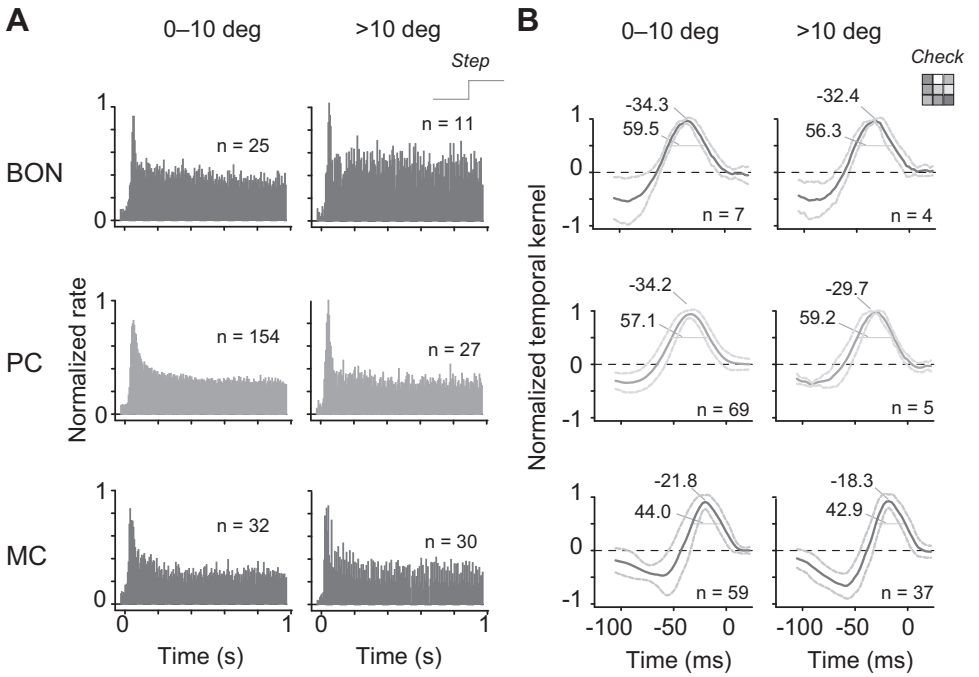

Fig. 6. Response time course, Step and Check stimuli. Normalized average responses to the Step stimulus (*A*) and the Check stimulus (*B*) for BON (*top*), PC (*middle*), and MC (*bottom*) cells. *A*: responses to achromatic (PC and MC, 90% contrast) and S cone-isolating (BON, 80% contrast) 0.5-Hz square wave. PSTH shows normalized average response time course for preferred contrast polarity, calculated as described in the text. *Left*: receptive field eccentricities below 10°. *Right*: eccentricities above 10°. *B*: normalized average temporal kernel (solid line) to achromatic (PC and MC) and S cone-isolating (BON) Check stimulus. For off-center cells the kernel was inverted before averaging. Dashed error lines show 1 SD. Horizontal lines show full width at half peak height.

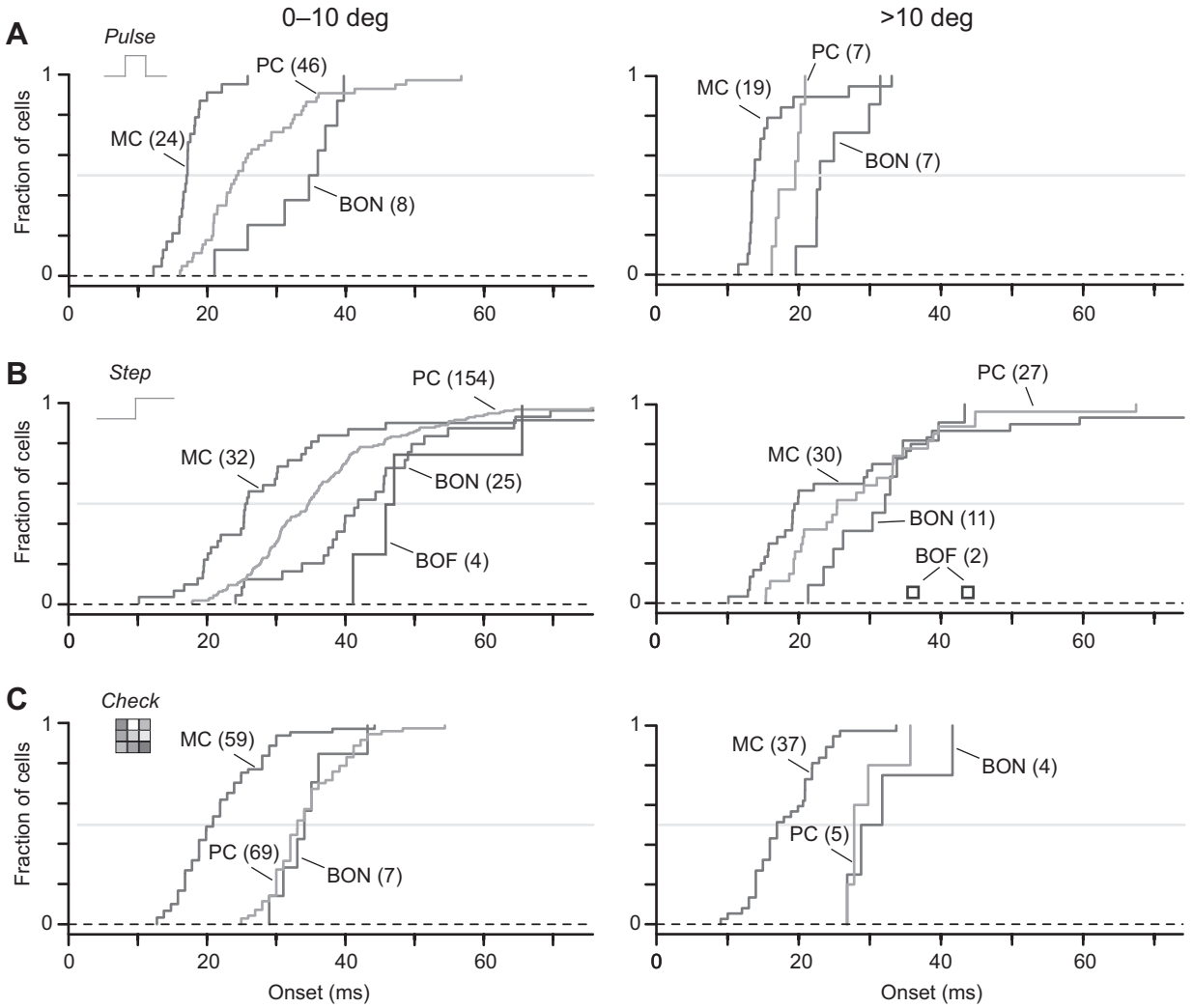

Fig. 7. Cumulative latency distribution. *A*: cumulative onset latency distribution for the Pulse stimulus. *Left*: receptive field eccentricities below 10°. *Right*: eccentricities above 10°. Intersection of each function with the gray horizontal line shows the median (50%) latency. Numbers in parentheses indicate group size. *B*: cumulative distribution for the Step stimulus. *C*: cumulative distribution for the Check stimulus.

BON populations show overall significant differences in response transience ($P < 0.02$). The MC cells showed the most transient response (FWHH: 43.6 ± 1.04 ms, $n = 96$). The FWHH values for PC cells (57.2 ± 1.05 ms, $n = 74$) and BON cells (58.4 ± 2.9 ms, $n = 11$) were significantly longer than the FWHH values for MC cells ($P < 0.02$). There was little difference between PC and BON cells ($P > 0.02$), or between central and peripheral samples, for any cell type ($P > 0.02$ for all comparisons). Furthermore, as noted above (see *Comparison of on-center and off-center cells*), we found no difference on comparing on-center and off-center PC or MC cells. We conclude that the temporally distinct properties of MC cells are largely preserved under white noise stimulation, but the differences between PC and BON populations are reduced.

Comparison of onset latencies. Figure 7 summarizes onset latencies for the three stimuli tested, by cumulative distribution functions. Median latencies are given in Table 2. A consistent pattern of response to the Pulse (Fig. 7*A*), Step (Fig. 7*B*), and Check (Fig. 7*C*) stimuli is immediately obvious. Overall there are significant between-group effects for each stimulus ($P < 0.02$). Furthermore, for each stimulus MC cells have the most rapid onset latency, followed by PC and then BON cells. For example, in response to the Pulse stimulus (Fig. 7*A*), the mean onset latency of central MC cells (17.3 ± 0.6 ms, $n = 24$) is shorter than that of central PC cells (26.9 ± 1.3 ms, $n = 46$, $P < 0.02$) but latency of central PC cells is only marginally shorter than that of central BON cells (35.7 ± 3.6 ms, $n = 8$, $P > 0.02$). The same progression, at shorter overall latencies, is present

Table 2. *Median latency*

Stimulus Type	Cell Type	0–10°	>10°
Pulse	MC	17.2	13.8
	PC	24.3	19.6
	BON	35.2	23.1
Step	MC	25.6	19.9
	PC	34.5	25.7
	BON	41.5	32.5
	BOF	46.5	40.2
Check	MC	20.9	16.9
	PC	32.9	27.9
	BON	33.9	30.4

Data are median onset latency to the 3 stimuli used in this study. Data are split into 2 eccentricity groups (0–10° and >10°).

in peripheral visual field (MC: 15.9 ± 1.3 ms, $n = 19$; PC: 18.7 ± 0.8 ms, $n = 8$, $P > 0.02$; BON: 25.0 ± 1.8 ms, $n = 7$, $P < 0.02$).

With Step and Pulse stimuli we see a consistent pattern emerging. In central visual field, latencies of MC cells to the Step stimulus (Fig. 7*B*) are shorter than latencies of PC cells and BON cells ($P < 0.02$); the PC cell latencies are also shorter than latencies of BON cells ($P < 0.02$). In common with responses to the Pulse stimulus, PC cell and BON cell latencies in peripheral field are shorter than those of their counterparts in central retina ($P < 0.02$); the MC cell latencies are also marginally shorter in peripheral than in central visual field ($P = 0.14$). Mean latency of a small number of BOF cells ($n = 4$) recorded with the Step stimulus (49.9 ± 6.2 ms) is longer than that of BON cells (46.9 ± 4.7 ms, $n = 25$, $P = 0.24$).

As shown in Fig. 7*C*, MC cell response latency to the Check stimulus in central visual field is shorter than that of PC and BON cells ($P < 0.02$), but there is little difference between PC and BON cells ($P = 0.86$). In common with responses to the Pulse and Step stimuli, response latency for the Check stimulus is reduced in peripheral visual field for PC cells ($P = 0.04$) and MC cells ($P < 0.02$); the difference for BON cells is less pronounced ($P = 0.35$), but the sample size is small.

The cumulative functions emphasize the influence of visual field eccentricity on visual response latency. In central visual field <20% of PC cells respond to the Pulse stimulus within 20 ms, whereas >90% of PC cells in peripheral retina do; in other words, the PC cell latency in the peripheral visual field is very similar to that of MC cells in the central visual field. We discuss these details further in DISCUSSION; for now the important point to take from Fig. 7 is that MC cells respond at shortest latency and BON and BOF cells generally are delayed relative to both MC and PC cells.

Comparison of dichromatic and trichromatic marmosets. Marmosets show polymorphic color vision, whereby males are obligate dichromats ("red-green color-blind") but many females express distinct M and L pigments separated by up to 20 nm peak sensitivity. Many PC cells in these trichromatic marmosets (like those in macaque monkeys) respond to red-green color contrast at low spatial frequency (Martin et al. 2011; Yeh et al. 1995b). We and others previously showed large differences in response timing among different classes of PC cells under red-green isoluminant or luminance modulation. For example, the "red-on" and "green-off" subgroups of PC cells respond in phase for red-green modulation but out of phase for luminance modulation (Kaplan and Benardete 2001; Kilavik et al. 2003; Lankheet et al. 1998; Martin et al. 2011; Smith et al. 1992). Thus PC cell timing should vary substantially across the various combinations of chromatic and luminance contrast in natural scenes. Furthermore, the low achromatic contrast sensitivity of PC cells has been taken as evidence that the PC receptive fields are specialized to detect red-green chromatic contrast at the expense of luminance contrast sensitivity (Lee et al. 2012; Shapley and Perry 1986). Because our database includes both dichromatic ($n = 14$) and trichromatic ($n = 6$) individuals with M and L pigments separated by 20 nm, we could ask whether expression of red-green color vision causes changes in response timing of PC pathway cells for achromatic stimuli (which modulate M and L cones in phase). The result for the Step stimulus is shown as a scatterplot in Fig. 8*A*. Here it is clear that there is heavy overlap of the dichromat and trichromat populations; comparison of latency for cells within 10° eccentricity (dichromat mean 36.2 ± 10.2 ms, $n = 54$; trichromat mean 33.0 ± 8.4 ms, $n = 65$, $P = 0.1$) confirms that expression of red-green color vision does not influence response latency for achromatic stimuli in PC cells. Latencies of the small number of BON cells ($n = 3$) recorded in trichromats are likewise not clearly distinct from those recorded in dichromats ($n = 19$; Fig. 8*B*), but the sample is too small for statistical comparison. These data add to other evidence that red-green color signals emerge as an additional response dimension, without changing the spatial or temporal properties of PC receptive fields (Conway et al. 2010; Martin et al. 2011; Mollon 1989).

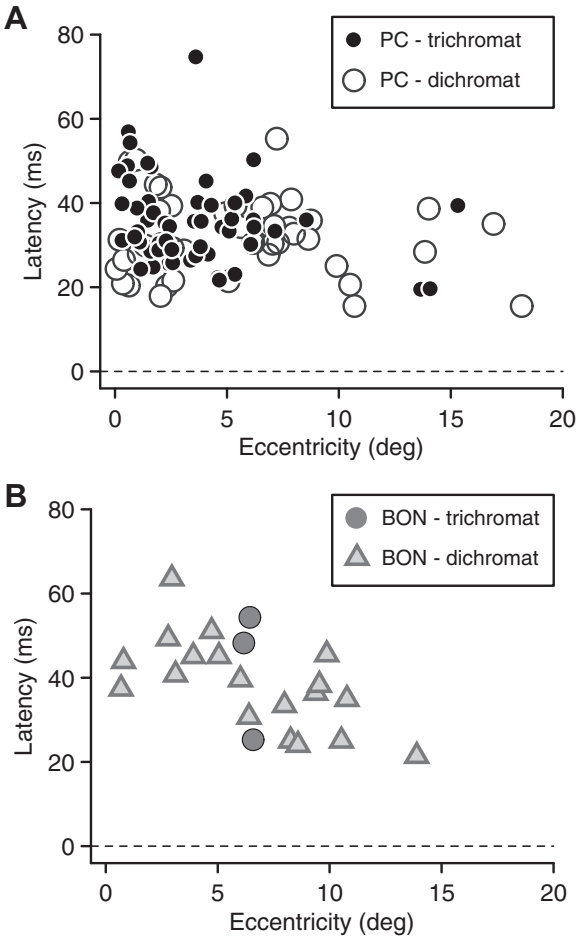

Fig. 8. Comparison of dichromatic and trichromatic marmosets. *A*: latency comparison of PC cells in dichromatic and trichromatic marmosets. *B*: latency comparison of BON cells in dichromatic and trichromatic marmosets. Note heavy overlap of latency distribution for PC and BON cells in dichromatic and trichromatic marmosets.

Latency correlations across visual stimuli. The results so far suggest that cell class (MC, PC, BON, BOF) is more important than stimulus type in determining response latency and time course: for their preferred stimulus MC cells respond most rapidly, followed by PC cells and then BON and BOF cells. If this is true, then our measures of latency and time course should be correlated across stimuli. For example, a cell that responds at short latency to the Pulse stimulus should also respond at short latency to the Step and Check stimuli. This hypothesis is supported by the data, as follows.

Figure 9*A* shows (for cells to which both stimuli were presented) a scatterplot of onset latency to Pulse and Step stimuli. Overall, there is strong positive correlation between the two measures ($r^2 = 0.53$, $n = 79$, $P < 0.02$); the within-class correlations were also high (PC: $r^2 = 0.51$, $n = 42$, $P < 0.02$; MC: $r^2 = 0.55$, $n = 24$, $P < 0.02$; BON: $r^2 = 0.33$, $n = 13$, $P < 0.02$). Nearly all data points lie below the unity line, indicating that the Step latency estimate is consistently longer than the Pulse latency estimate. The reason for this difference is unclear; the asymmetric adaptation take-off point for the Step stimulus noted above (see MATERIALS AND METHODS) may play a role, but we did not study this question in more detail. Furthermore, the regression line slope is <1 (0.60; Fig. 9*A*), indicating that the difference grows with increasing latency (possibly because the shortest latency responses to Pulse stimuli approach a minimum bound). A broadly consistent result is seen on comparing onset latencies for Check and Step stimuli (Fig. 9*B*; overall: $r^2 = 0.39$, $n = 55$, $P < 0.02$; PC: $r^2 = 0.40$, $n = 34$, $P < 0.02$; MC: $r^2 = 0.08$, $n = 17$, $P = 0.27$; BON: $r^2 = 1.00$, $n = 4$, $P < 0.02$). Here, however, the slope of the regression line is close to unity (1.03; Fig. 9*B*), indicating that the Step latency estimate is simply a temporal translation of the Check latency estimate. Finally we show (Fig. 9*C*) that the onset latency for preferred (on or off) contrast pulses is strongly correlated with the offset response latency for anti-preferred polarity (where identical cone adaptation conditions prevail for all cell types over the response time course). All these results provide further evidence that the timing differences between PC, MC, and BON cells can be reasonably expected to apply across a range of spatial stimulus configurations presented on a CRT monitor.

Opponent inputs to BON cells. It is well known that BON cells show "blue-on, yellow-off" cone opponent responses (DeValois et al. 1966; Dreher et al. 1976; Tailby et al. 2008b; Wiesel and Hubel 1966). In foregoing sections we showed that blue-on (S cone mediated) responses in BON cells lag the (ML cone mediated) responses of MC and PC cells. If the ML cone pathways feeding the yellow-off input to BON cells have the same temporal properties as those feeding MC and PC cells, we would thus expect them to arrive before the blue-on responses. Previous data, however, suggested that yellow-off responses in BON cells arrive simultaneous to (or later than) blue-on responses (Crook et al. 2009; Field et al. 2007; Yeh et al. 1995a). We therefore measured and compared latency of S and ML inputs to BON cells. Figure 10*A* shows the response of an example BON cell to S cone increment Pulse stimulus. The more sluggish onset and slower rise of response to the cone opponent stimulus (ML decrement, presented at the same cone contrast as the S cone increment) are apparent in Fig. 10*B*. Overall, we found that the response of BON cells to the ML-isolating pulse is slower (49.2 ± 5.3, $n = 14$) than to the S-isolating pulse (28.7 ± 1.9, $n = 14$, $P < 0.02$). That ML-off latency is longer and more variable than S-on latency is also apparent in Fig. 10*E*, where the data points form a horizontally elongated cloud to the right of the unity line. To ensure that the long response latency for ML stimuli is not due to artifactual S-cone contrast in the presumed cone-isolating ML stimulus, we also compared latency for achromatic and ML-isolating pulses in MC and PC cells (Fig. 10*D*). Here the data cluster around the unity line. This result indicates that there is little or no contamination of the ML cone-isolating pulses by S cones,

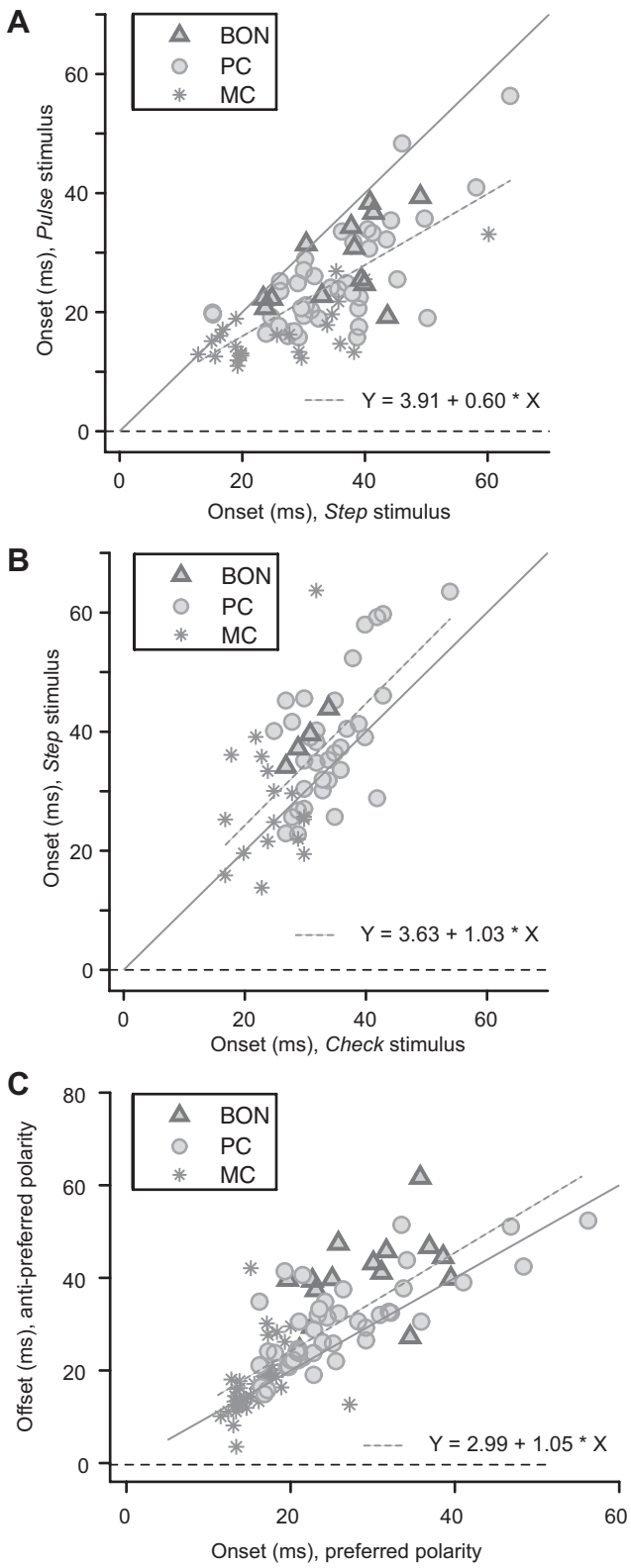

Fig. 9. Stimulus type comparison. Onset latency comparison between stimuli. *A*: comparison between the onset latency of the Pulse and Step stimuli. Black line is the unity line. Dashed line shows linear regression of all cells (correlation coefficient = 0.73, $r^2 = 0.53$, $P < 0.02$, $n = 79$). *B*: comparison between Step and Check stimuli. Correlation coefficient = 0.63, $r^2 = 0.39$, $n = 55$, $P < 0.02$. *C*: comparison between onset latency of the preferred and offset of the antipreferred polarity for the Pulse stimulus. Correlation coefficient = 0.77, $r^2 = 0.59$, $n = 102$, $P < 0.02$. Other details as in *A*.

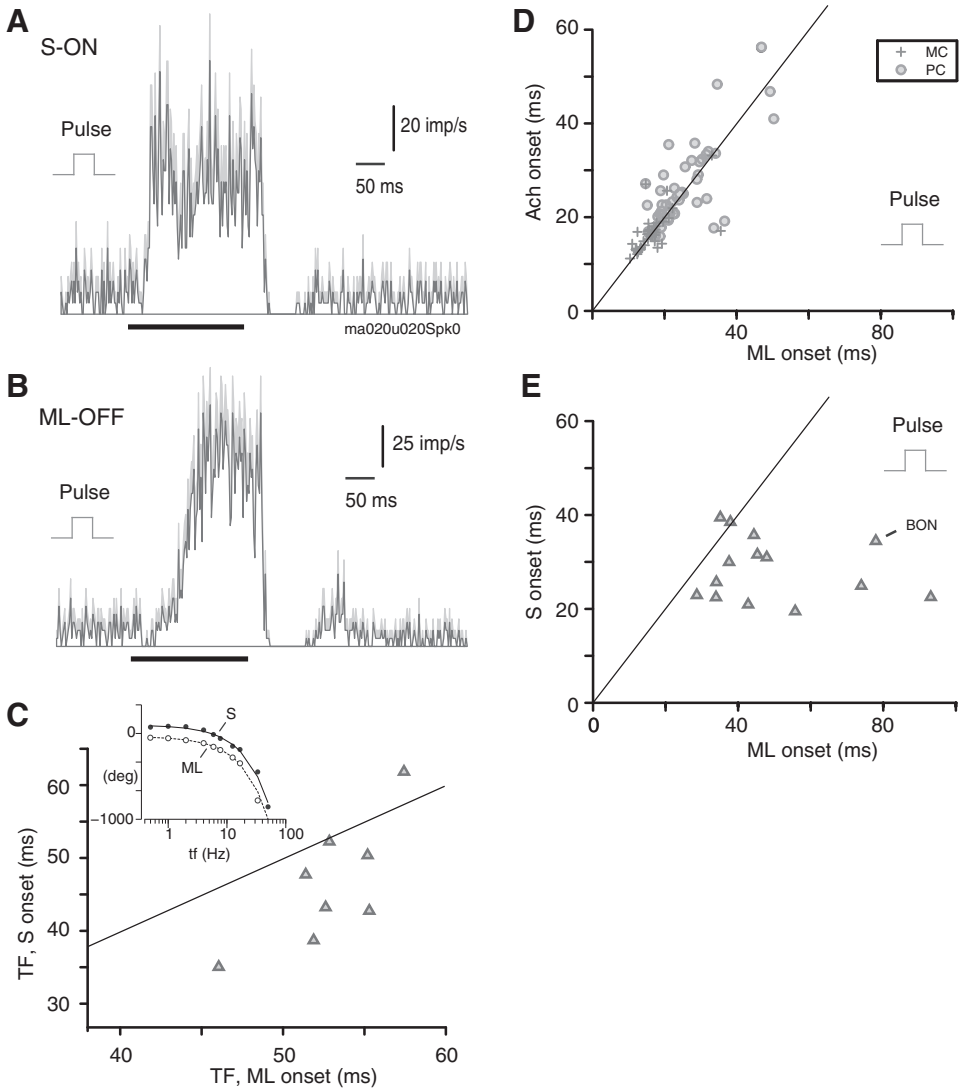

Fig. 10. Cone-opponent latency in BON cells. *A*: example of the response of a BON cell to its preferred S-ON stimulus using the Pulse protocol. The black bar indicates when the stimulus was present. *B*: response of the same BON cell to the cone opponent ML-OFF stimulus. Note the slower time course compared with the preferred stimulus in *A*. *C*: response latency to the S-ON and ML-OFF stimuli inferred from response phase regression on sinusoidal temporal frequency (TF) modulation of uniform fields. *Inset* shows phase-frequency relation for 1 cell. *D*: response latency of PC and MC cells to their preferred achromatic (Ach) and ML cultured stimuli in the Pulse protocol ($n = 96$). *E*: response latency of BON cells to the preferred S-ON and cone opponent ML-OFF stimulus using the Pulse protocol. The response to ML-off stimulus is consistently slower than the response to the S-ON stimulus. The solid line is the unity line in *C*–*E*.

because the ML-isolating stimulus produces the same response as the achromatic stimulus (which activates S cones as well as ML cones). For a subset of BON cells ($n = 8$) we further estimated latency from the response phase slope, using sinusoidal temporal modulation of spatially uniform S or ML selective fields (Fig. 10*C*). With this method the equivalent ML peak response time (52.8 ± 1.3 ms) is longer than the S peak response time (46.5 ± 3.3 ms, $P < 0.05$), but the difference between the two measures (~7 ms) is considerably less than the difference estimated from response onset for pulsed stimuli (~20 ms).

Frame-locking. One of the best-known characteristics of MC cells is their high sensitivity to flicker and rapid image motion. This high sensitivity can cause MC cell spiking to entrain to the frame refresh rate of a CRT monitor screen ("frame-locking") (Derrington et al. 1984; Lehky and Maunsell 1996). A quantitative comparison of frame-locking across LGN cell classes has not been made previously. Human sensitivity to high-temporal-frequency flicker increases with eccentricity from the fovea (Snowden and Hess 1992; Tyler 1985), as does the flicker sensitivity of macaque retinal ganglion cells (Solomon et al. 2002a). These results raise the question of how frame-locking depends on receptive field eccentricity. We characterized frame-locking with a simple metric (normalized power in the PSTH at the monitor refresh rate) in the period 75–175 ms after onset of the Pulse stimulus (see Fig. 11, *A* and *B*).

The results are summarized in Fig. 11, *C*–*E*. Overall, there is a significant difference in frame-locking across MC, PC, and BON cells ($P < 0.02$). Post hoc comparison reveals that in central visual field MC cells show greater frame-locking (0.28 ± 0.04; $n = 24$) than PC (0.15 ± 0.02; $n = 46$, $P < 0.05$) and BON (0.10 ± 0.03; $n = 8$, $P < 0.05$) cells. There was, however, little difference between PC and BON cells ($P = 0.60$). In peripheral visual field we see the same pattern: MC cells show greater frame-locking (0.57 ± 0.04; $n = 19$) than PC cells (0.30 ± 0.08; $n = 7$, $P < 0.05$) and BON cells (0.08 ± 0.01; $n = 7$, $P < 0.05$). Consistently, in PC and MC cell groups frame-locking increases with eccentricity (PC: $r^2 = 0.31$, $P < 0.02$, Fig. 11*C*; MC: $r^2 = 0.46$, $P < 0.02$, Fig. 11*D*). There is no detectable influence of eccentricity on frame-locking in BON cells ($r^2 = 0.003$, $P = 0.86$, Fig. 11*E*), but the range of eccentricities measured is smaller for BON cells than for PC or MC cells. We conclude that high-frequency entrainment in LGN is strongest in MC cells and weakest in BON cells. One implication of this result is that video-rate entrainment of cortical signals (Dhruv et al.

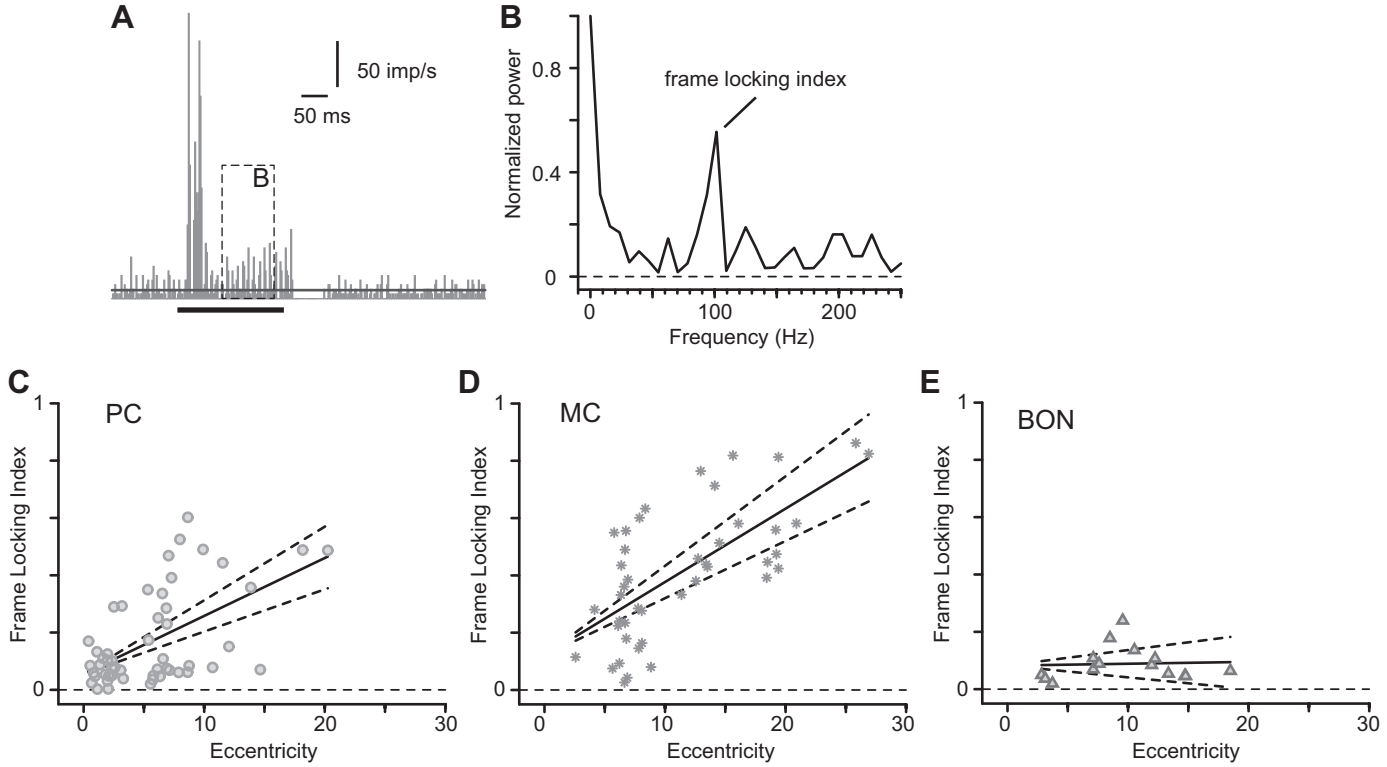

Fig. 11. Frame-locking. *A*: PSTH response of an MC cell to a Pulse stimulus with 2-ms bin size. The horizontal bar below the PSTH indicates the stimulus duration. Maintained discharge rate is indicated by thin black line. Dashed lines show the region of the PSTH that was analyzed to assess frame-locking. *B*: normalized fast Fourier transform showing 75 ms to 175 ms stimulus. The bin including 100 Hz (monitor refresh rate) is taken as a measure of frame-locking. *C–E*: scatterplots of frame-locking index (Fourier power at CRT frame refresh frequency) set out against cell eccentricity for PC cells (*C*), MC cells (*D*), and koniocellular BON cells (*E*). Solid lines show linear regression; dashed lines show 95% confidence intervals. Note that for PC and MC cells frame-locking becomes more pronounced with increased eccentricity, while there is negligible change for BON cells.

2009; Krolak-Salmon et al. 2003; Williams et al. 2004) is primarily a result of MC pathway activity.

DISCUSSION

Our main findings are that visual evoked responses in marmoset LGN arise fastest in MC cells and slowest in BON and BOF cells and that BON responses show more sustained temporal characteristics than MC or PC responses. In the following we consider sources of latency differences in parallel subcortical pathways and ask how the distinct temporal signatures in parallel pathways arise.

Retinal and central contributions to response latency. The chief contributors to visual response latency in LGN are *1*) intraretinal delay between visual stimulus onset and changes in ganglion cell spike rate and *2*) retino-geniculate delay between ganglion cell spike and LGN spike. Taking, for example, the onset latency to Pulse stimuli in central visual field (MC, ~17 ms; PC, ~27 ms; BON, ~36 ms), we can make a rough estimate of the relative contribution of these delays. Measured antidromic and orthodromic evoked latencies of MC, PC, and KC cells in macaque retina (Solomon et al. 2005), macaque LGN, and *Galago* LGN (Dreher et al. 1976; Irvin et al. 1986) yield retino-geniculate conduction times of ~4 ms for MC cells, ~7 ms for PC cells, and ~9 ms for KC cells. The inferred delay from visual stimulation to ganglion cell spiking would therefore be ~13 ms in MC cells, ~20 ms in PC cells, and ~27 ms in KC cells. Thus, as predicted by analogy with studies of parallel pathways in cat retina (Cleland et al. 1976), timing delays between parallel pathways in primates begin in the retina. In principle, the contribution of intraretinal axon path lengths to overall latency difference could be studied by comparing cells at equivalent eccentricities in nasal and temporal retina, but our Pulse data set was not large enough to support such analysis.

What factors could influence retinal delays? One possibility is that under our adaptation conditions S-cone excitation is lower than ML-cone excitation and therefore phototransduction will be slower in S cones than in ML cones. Indeed, the calculations described in MATERIALS AND METHODS predict that relative S-cone excitation at the background luminance is lower than that of ML cones (S-to-ML ratio is ~9%). However, the high background intensity we used (equivalent to ~1,500 Td) means that for all cone types the adaptation state is above the levels where phototransduction is retarded (Field et al. 2009; Lamb 2011; Schnapf et al. 1990). Thus this first possibility can be ruled out. Differential delay at the photoreceptor-bipolar synapse is a second possibility. The on-center bipolar cells are thought to express the same metabotropic glutamate receptor class 6 (mGluR6; see, for example, Vardi et al. 2000). However, by analogy with established differences between rod and cone bipolar cells (Berntson and Taylor 2000; Dunn et al. 2007), the postsynaptic response kinetics could differ among the (at least 9 distinct) bipolar classes feeding parallel retinal pathways. Distinct expression by off-bipolar cells expressing ionotropic glutamate (AMPA) and kainate receptors is proposed to underlie sustained and transient channels in ground

squirrel retina (DeVries 2000), but these possibilities have not been addressed in physiological studies of primate retina. Because our experiments were carried out at a single photopic adaptation level, we do not know how well the response timing and time course differences between parallel pathways are preserved under changes in background luminance (for discussion, see Lee et al. 1990; Martin and Solomon 2013; Maunsell et al. 1999; Stockman et al. 2006).

Are there timing differences between on-center and off-center pathways? We did not detect any onset latency (Fig. 3) or time to peak (data not shown) difference between on- and off-center cells in MC or PC classes; these results are consistent with previous in vivo studies (Lankheet et al. 1998; Martin et al. 2011; Yeh et al. 1995a) and suggest that temporal differences in metabotropic versus ionotropic receptor pathways are negligible compared with the relatively long time constants imposed by the phototransduction cascade (Schnapf et al. 1990; for example, see Fig. 3 in Koike et al. 2010). In this context it is important to recall that the mGluR6 transduction kinetics are orders of magnitude more rapid than those of other metabotropic glutamate receptor classes (Koike et al. 2010; Nakanishi 1992), which implies that rapid and symmetric response timing between on- and off-center cells is an important functional requirement for the mammalian visual system.

To add to this discussion of on-center and off-center pathways, the reader should note the following subtle technical point applying to stimuli presented on a CRT monitor. Because phosphor decay time is shorter than the interframe interval, intensity decrements displayed on a CRT monitor can be time-advanced by up to 5 ms relative to intensity increments (Gawne and Woods 2003; Zele and Vingrys 2005). The physical asymmetry in the stimulus could mask a small genuine lag in off-center cells relative to on-center cells. This limitation of CRT technology could help account for the (sub-ten millisecond) time advance of off-type responses relative to on-type responses in cat visual cortex (Jin et al. 2011; but see also Komban et al. 2014). It is notable that the temporal advantage in visual search for decrement compared with equal-sized increment targets is much longer, of the order of 0.2 s (Komban et al. 2011).

The shortest latencies we measured (in peripheral MC cells, 10–15 ms; Figs. 3, 4, 8, 9) are consistent with the shortest latencies (~15 ms) estimated by Maunsell et al. (1999) in one of two macaques, studied with stimulus and analysis methods very similar to those we used here. Other studies generally report longer latencies in macaque LGN, with a consistent 5–15 ms longer onset of PC cells relative to MC cells (35 vs. 23 ms, Schmolesky et al. 1998; 44 vs. 38 ms, Levitt et al. 2001; 38 vs. 25 ms and 25 vs. 18 ms, Maunsell et al. 1999). Thus although absolute latency estimates do vary (at least partly a consequence of different studies using different methods and different statistical criteria to determine latency), there is good agreement that PC responses lag MC responses by ~10 ms. It remains untested whether the shorter latencies in marmoset compared with macaque are simply attributable to the (relatively) tiny size of a marmoset's brain, but this seems a likely explanation.

In sum, when visual signals leave the LGN there is already a significant lag in latency between cells receiving signals from S cones and cells receiving inputs from L and M cones. The lag (10–20 ms) is consistent with psychophysical measurements (Lee et al. 2009; McKeefry et al. 2003). As pointed out previously (Smithson and Mollon 2004) the lag in S-cone signals leaving the LGN is, however, only about half the delay of S-cone inputs to many cortical cells reported by Cottaris and De Valois (1998). Notwithstanding this question, our data do show that the (red-green) chromatic signals carried by PC cells will arrive at the cortex before the (blue-yellow) signals carried by KC cells. The time integration window of subsequent processing stages must be broad enough to cover this delay.

Temporal signatures of parallel pathways. From the studies cited above there is broad agreement on the following differences between MC and PC pathway cells. First, MC responses to flashed stimuli lead PC responses by 10–20 ms and are more transient than PC responses. Second, MC responses to sine-wave temporal modulation extend to higher temporal frequencies than PC responses do. Finally, the spike-triggered average stimulus time course of MC cells is faster and shows a shorter integration time than that of PC cells. Our results add BON and BOF cells to this pattern, as follows. Compared with MC and PC responses, BON and BOF responses show longest latency (Figs. 3, 4, 7), are most sustained (Fig. 6*A*), and show the slowest spike-triggered average stimulus time course (Fig. 6*B*). In these respects the visual evoked response properties of BON cells can all be described as more sluggish than those of MC and PC pathways. This result is consistent with proposed homologies of the KC pathways and "sluggish-W" pathways delineated in the cat visual system. Although the term "sluggish" originally referred to slow axonal conduction velocity (Cleland et al. 1976), our results are consistent with the customary broader description taking account of visual evoked response properties of sluggish-W pathways (Casagrande and Xu 2003; Smithson and Mollon 2004). Our results are likewise consistent with previous studies showing slow and variable onset latencies of KC cells in nocturnal primates (Casagrande and Xu 2003; Irvin et al. 1986). These species lack S cones entirely, meaning that there must be reasons other than color coding to account for slow temporal dynamics of KC cells (for review, see Casagrande and Xu 2003). As noted above, where measured the KC populations tend to show relatively slow axon conduction velocity as well as slow visual evoked responses.

Although our sample of BOF receptive fields is small, the BOF latency was consistently longer than that of any other cell class. This result is consistent with evidence that anatomical pathways feeding BON and BOF responses are distinct from those feeding PC and MC responses (reviewed by Miyagishima et al. 2014).

Opponent inputs to BON cells. We found that the yellow-off (ML) cone inputs to BON cells are delayed by ~20 ms relative to the blue-on (S) cone inputs (~60 vs. ~40 ms; Fig. 10). The source of this delay and its physiological impact are unclear. Although all studies agree that the ML inputs are never faster than S inputs, there is poor agreement between laboratories on the delay time. Yeh et al. (1995a) reported no delay between S-on and ML-off responses in macaque retina recordings in vivo, Crook et al. (2009) report ~6-ms delay in in vitro macaque recordings, and Tailby et al. (2008a) report ~6-ms delay in recordings from macaque LGN. By contrast, Chichilnisky and coworkers (Chichilnisky and Baylor 1999; Field et al. 2007) report delays of ~15–20 ms in in vitro macaque retinal recordings, and Reid and Shapley (1992) and Gielen et al. (1982) report 15–20 ms delay between ML and S inputs to

blue-on cells in macaque LGN. Among the studies cited, shorter delays are obtained where latency is inferred by regression of response phase from temporal frequency modulation, whereas measurements from spike-triggered average ("checkerboard") stimulation yield longer delays. Consistently, we measured shorter delays (~7 ms) under temporal frequency modulation compared with the Pulse stimulus.

What is the cause of the stimulus-dependent differences described above? The Pulse and Check stimuli comprise temporal step modulations and thus a much broader spectrum of temporal frequencies than does sine-wave temporal modulation (i.e., single temporal frequency, in our case 5 Hz). High temporal frequencies can drive rapid feedforward inhibition in the retina (Murphy and Rieke 2008; Solomon et al. 2006) and thalamus (Lorincz et al. 2009). We have shown previously that suppressive surrounds of BON cells in LGN are predominantly driven by ML cone signals (Solomon et al. 2002b; Tailby et al. 2008b). If rapid inhibition is likewise biased to ML cones, it could suppress an early component of the ML response but leave the S cone response unaffected.

Frame-locking. We saw substantial frame-locking in responses of MC cells, weak frame-locking in peripheral PC cells, and little sign of frame-locking in BON cells. Our observations extend sporadic previous reports by showing a clear relation of frame-locking to receptive field eccentricity. Derrington et al. (1984) reported frame-locking at refresh rates of 60 Hz in MC but not PC cells in macaque LGN. Williams et al. (2004) reported, without showing data, frame-locking of local field potential in LGN of macaque at 60 Hz (but not at 120 Hz). Krolak-Salmon et al. (2003) reported entrainment of local field potential in human LGN at 70-Hz refresh rate. Stronger frame-locking in peripheral receptive fields is consistent with the known increase in sensitivity to high temporal frequencies in peripheral macaque retina (Solomon et al. 2002a, 2005), which in turn may reflect faster integration time in the photoreceptors (Tyler 1985). The fact that BON cells do not show frame-locking implies that S cones and/or the postreceptoral circuitry filters out high temporal frequencies. Frame-locking was not present in the ML-off response of BON cells (data not shown), demonstrating that the filtering site for the off response must be downstream of the ML photoreceptors. Consistently, the high frequency sensitivity of BON cells is lower than that of PC cells (Tailby et al. 2008a; Yeh et al. 1995a). We speculate that the substantial segregation of frame-locking to MC cells might be exploitable in human physiological measurements (for example, visual evoked potentials) as a signature of MC pathway inputs.

ACKNOWLEDGMENTS

We thank A. Demir and C. Guy for technical assistance, S. Gharaei, P. Romo, S. S. Solomon (no relation to S. G. Solomon), and N. Zeater for assistance with data collection, and B. Dreher for helpful comments and discussion.

GRANTS

This work was supported by an Australian National Health and Medical Research Council grant (1027913) and an Australian Research Council grant (CE140100007).

DISCLOSURES

No conflicts of interest, financial or otherwise, are declared by the author(s).

AUTHOR CONTRIBUTIONS

Author contributions: A.N.P., S.G.S., and P.R.M. conception and design of research; A.N.P., S.K.C., S.G.S., C.T., and P.R.M. performed experiments; A.N.P., S.K.C., S.G.S., C.T., and P.R.M. analyzed data; A.N.P., S.K.C., S.G.S., C.T., and P.R.M. interpreted results of experiments; A.N.P. and P.R.M. prepared figures; A.N.P. and P.R.M. drafted manuscript; A.N.P., S.K.C., S.G.S., C.T., and P.R.M. edited and revised manuscript; A.N.P., S.K.C., S.G.S., C.T., and P.R.M. approved final version of manuscript.

REFERENCES

Berntson A, Taylor WR. Response characteristics and receptive field widths of on-bipolar cells in the mouse retina. *J Physiol* 524: 879–889, 2000.

Brindley GS, Du Croz JJ, Rushton WA. The flicker fusion frequency of the blue-sensitive mechanism of colour vision. *J Physiol* 183: 497–500, 1966.

Bullier J, Henry GH. Ordinal position and afferent input of neurons in monkey striate cortex. *J Comp Neurol* 193: 913–935, 1980.

Casagrande VA, Xu X. Parallel visual pathways: a comparative perspective. In: *The Visual Neurosciences*, edited by Chalupa LM, Werner JS. Cambridge, MA: MIT Press, 2003, p. 494–506.

Chen S, Li W. A color-coding amacrine cell may provide a blue-off signal in a mammalian retina. *Nat Neurosci* 15: 954–956, 2012.

Cheong SK, Tailby C, Martin PR, Levitt JB, Solomon SG. Slow intrinsic rhythm in the koniocellular visual pathway. *Proc Natl Acad Sci USA* 108: 14659–14663, 2011.

Cheong SK, Tailby C, Solomon SG, Martin PR. Cortical-like receptive fields in the lateral geniculate nucleus of marmoset monkeys. *J Neurosci* 33: 6864–6876, 2013.

Chichilnisky EJ. A simple white noise analysis of neuronal light responses. *Network* 12: 199–213, 2001.

Chichilnisky EJ, Baylor DA. Receptive-field microstructure of blue-yellow ganglion cells in primate retina. *Nat Neurosci* 2: 889–893, 1999.

Chichilnisky EJ, Kalmar RS. Functional asymmetries in ON and OFF ganglion cells of primate retina. *J Neurosci* 22: 2737–2747, 2002.

Cleland BG, Levick WR, Morstyn R, Wagner HG. Lateral geniculate relay of slowly-conducting retinal afferents to cat visual cortex. *J Physiol* 255: 299–320, 1976.

Conway BR, Chatterjee S, Field GD, Horwitz GD, Johnson EN, Koida K, Mancuso K. Advances in color science: from retina to behavior. *J Neurosci* 30: 14955–14963, 2010.

Cottaris NP, DeValois RL. Temporal dynamics of chromatic tuning in macaque primary visual cortex. *Nature* 395: 896–900, 1998.

Croner LJ, Kaplan E. Receptive fields of P and M ganglion cells across the primate retina. *Vision Res* 35: 7–24, 1995.

Crook JD, Davenport CM, Peterson BB, Packer OS, Detwiler PB, Dacey DM. Parallel ON and OFF cone bipolar inputs establish spatially coextensive receptive field structure of blue-yellow ganglion cells in primate retina. *J Neurosci* 29: 8372–8387, 2009.

Dacey DM, Lee BB. The "blue-on" opponent pathway in primate retina originates from a distinct bistratified ganglion cell type. *Nature* 367: 731–735, 1994.

de Lange DZ. Research into the dynamic nature of the human fovea-cortex systems with intermittent and modulated light. I. Attenuation characteristics with white and colored light. *J Opt Soc Am* 48: 777–784, 1958.

Derrington AM, Krauskopf J, Lennie P. Chromatic mechanisms in lateral geniculate nucleus of macaque. *J Physiol* 357: 241–265, 1984.

DeValois RL, Abramov I, Jacobs GH. Analysis of response patterns of LGN cells. *J Opt Soc Am* 56: 966–977, 1966.

DeVries SH. Bipolar cells use kainate and AMPA receptors to filter visual information into separate channels. *Neuron* 28: 847–856, 2000.

Dhruv NT, Tailby C, Sokol SH, Majaj NJ, Lennie P. Nonlinear signal summation in magnocellular neurons of the macaque lateral geniculate nucleus. *J Neurophysiol* 102: 1921–1929, 2009.

Dreher B, Fukada Y, Rodieck RW. Identification, classification and anatomical segregation of cells with X-like and Y-like properties in the lateral geniculate nucleus of Old-World primates. *J Physiol* 258: 433–452, 1976.

Dunn FA, Lankheet MJ, Rieke F. Light adaptation in cone vision involves switching between receptor and post-receptor sites. *Nature* 449: 603–607, 2007.

Enroth-Cugell C, Robson J. The contrast sensitivity of retinal ganglion cells of the cat. *J Physiol* 187: 517–552, 1966.

Field GD, Greschner M, Gauthier JL, Rangel C, Shlens J, Sher A, Marshak DW, Litke AM, Chichilnisky EJ. High-sensitivity rod photore-

ceptor input to the blue-yellow color opponent pathway in macaque retina. *Nat Neurosci* 12: 1159–1164, 2009.

Field GD, Sher A, Gauthier JL, Greschner M, Shlens J, Litke AM, Chichilnisky EJ. Spatial properties and functional organization of small bistratified ganglion cells in primate retina. *J Neurosci* 27: 13261–13272, 2007.

Gawne TJ, Woods JM. Video-rate and continuous visual stimuli do not produce equivalent response timings in visual cortical neurons. *Vis Neurosci* 20: 495–500, 2003.

Gielen CC, van Gisbergen JA, Vendrik AJ. Reconstruction of cone-system contributions to responses of colour-opponent neurones in monkey lateral geniculate. *Biol Cybern* 44: 211–221, 1982.

Gouras P, Zrenner E. Enhancement of luminance flicker by color-opponent mechanisms. *Science* 205: 587–589, 1979.

Haverkamp S, Grünert U, Wässle H. The synaptic architecture of AMPA receptors at the cone pedicle of the primate retina. *J Neurosci* 21: 2488–2500, 2001.

Hendry SH, Reid RC. The koniocellular pathway in primate vision. *Annu Rev Neurosci* 23: 127–153, 2000.

Irvin GE, Norton TT, Sesma MA, Casagrande VA. W-like response properties of interlaminar zone cells in the lateral geniculate nucleus of a primate (*Galago crassicaudatus*). *Brain Res* 362: 254–270, 1986.

Jin J, Wang Y, Lashgari R, Swadlow HA, Alonso JM. Faster thalamocortical processing for dark than light visual targets. *J Neurosci* 31: 17471–17479, 2011.

Kaplan E, Benardete E. The dynamics of primate retinal ganglion cells. *Prog Brain Res* 134: 17–34, 2001.

Kaplan E, Shapley RM. The primate retina contains two types of ganglion cells, with high and low contrast sensitivity. *Proc Natl Acad Sci USA* 83: 2755–2757, 1986.

Kilavik BE, Silveira LC, Kremers J. Centre and surround responses of marmoset lateral geniculate neurones at different temporal frequencies. *J Physiol* 546: 903–919, 2003.

Klug K, Herr S, Ngo IT, Sterling P, Schein S. Macaque retina contains an S-cone OFF midget pathway. *J Neurosci* 23: 9881–9887, 2003.

Koike C, Obara T, Uriu Y, Numata T, Sanuki R, Miyata K, Koyasu T, Ueno S, Funabiki K, Tani A, Ueda H, Kondo M, Mori Y, Tachibana M, Furukawa T. TRPM1 is a component of the retinal ON bipolar cell transduction channel in the mGluR6 cascade. *Proc Natl Acad Sci USA* 107: 332–337, 2010.

Komban SJ, Alonso JM, Zaidi Q. Darks are processed faster than lights. *J Neurosci* 31: 8654–8658, 2011.

Komban SJ, Kremkow J, Jin J, Wang Y, Lashgari R, Li X, Zaidi Q, Alonso JM. Neuronal and perceptual differences in the temporal processing of darks and lights. *Neuron* 82: 224–234, 2014.

Kremers J, Lee BB, Pokorny J, Smith VC. Responses of macaque ganglion cells and human observers to compound periodic waveforms. *Vision Res* 33: 1997–2011, 1993.

Krolak-Salmon P, Henaff MA, Tallon-Baudry C, Yvert B, Guenot M, Vighetto A, Mauguiere F, Bertrand O. Human lateral geniculate nucleus and visual cortex respond to screen flicker. *Ann Neurol* 53: 73–80, 2003.

Lamb TD. Photoreceptor spectral sensitivities: common shape in the long-wavelength region. *Vision Res* 35: 3083–3091, 1995.

Lamb TD. Light adaptation in photoreceptors. In: *Adler's Physiology of the Eye* (11th ed.), edited by Levin LA, Nilsson SF, Ver Hoeve J, Wu S, Kaufman PL, Alm A. Edinburgh: Elsevier, 2011, p. 429–442.

Lankheet MJ, Lennie P, Krauskopf J. Distinctive characteristics of subclasses of red-green P-cells in LGN of macaque. *Vis Neurosci* 15: 37–46, 1998.

Lee BB, Martin PR, Grünert U. Retinal connectivity and primate vision. *Prog Retin Eye Res* 29: 622–639, 2010.

Lee BB, Pokorny J, Smith VC, Kremers J. Responses to pulses and sinusoids in macaque ganglion cells. *Vision Res* 34: 3081–3096, 1994.

Lee BB, Pokorny J, Smith VC, Martin PR, Valberg A. Luminance and chromatic modulation sensitivity of macaque ganglion cells and human observers. *J Opt Soc Am A* 7: 2223–2236, 1990.

Lee BB, Shapley RM, Hawken MJ, Sun H. Spatial distributions of cone inputs to cells of the parvocellular pathway investigated with cone-isolating gratings. *J Opt Soc Am A Opt Image Sci Vis* 29: A223–A232, 2012.

Lee RJ, Mollon JD, Zaidi Q, Smithson HE. Latency characteristics of the short-wavelength-sensitive cones and their associated pathways. *J Vis* 9: 1–17, 2009.

Lehky SR, Maunsell JH. No binocular rivalry in the LGN of alert macaque monkeys. *Vision Res* 36: 1225–1234, 1996.

Lennie P, Movshon JA. Coding of color and form in the geniculostriate visual pathway. *J Opt Soc Am A Opt Image Sci Vis* 22: 2013–2033, 2005.

Levitt JB, Shumer RA, Sherman SM, Spear PD. Visual response properties of neurons in the LGN of normally reared and visually deprived macaque monkeys. *J Neurophysiol* 85: 2111–2119, 2001.

Lorincz ML, Kekesi KA, Juhasz G, Crunelli V, Hughes SW. Temporal framing of thalamic relay-mode firing by phasic inhibition during the alpha rhythm. *Neuron* 63: 683–696, 2009.

Martin PR, Blessing EM, Buzás P, Szmajda BA, Forte JD. Transmission of colour and acuity signals by parvocellular cells in marmoset monkeys. *J Physiol* 589: 2795–2812, 2011.

Martin PR, Solomon SG. Spike timing in the early stages of visual processing. In: *Spike Timing: Mechanisms and Function*, edited by DiLorenzo P, Victor JD. New York: Taylor & Francis, 2013, p. 343–373.

Maunsell JH, Ghose GM, Assad JA, McAdams CJ, Boudreau CE, Noerager BD. Visual response latencies of magnocellular and parvocellular LGN neurons in macaque monkeys. *Vis Neurosci* 16: 1–14, 1999.

McKeefry DJ, Parry NR, Murray IJ. Simple reaction times in color space: the influence of chromaticity, contrast, and cone opponency. *Invest Ophthalmol Vis Sci* 44: 2267–2276, 2003.

Merigan WH, Maunsell JH. How parallel are the primate visual pathways? *Annu Rev Neurosci* 16: 369–402, 1993.

Miyagishima KJ, Grünert U, Li W. Processing of S-cone signals in the inner plexiform layer of the mammalian retina. *Vis Neurosci* 31: 153–163, 2014.

Mollon JD. "Tho' she kneel'd in the place where they grew." The uses and origins of primate colour vision. *J Exp Biol* 146: 21–38, 1989.

Murphy GJ, Rieke F. Signals and noise in an inhibitory interneuron diverge to control activity in nearby retinal ganglion cells. *Nat Neurosci* 11: 318–326, 2008.

Nakanishi S. Molecular diversity of glutamate receptors and implications for brain function. *Science* 258: 597–603, 1992.

Reid RC, Shapley RM. Spatial structure of cone inputs to receptive fields in primate lateral geniculate nucleus. *Nature* 356: 716–718, 1992.

Schmolesky MT, Wang Y, Hanes DP, Thompson KG, Leutgeb S, Schall JD, Leventhal AG. Signal timing across the macaque visual system. *J Neurophysiol* 79: 3272–3278, 1998.

Schnapf JL, Nunn BJ, Meister M, Baylor DA. Visual transduction in cones of the monkey (*Macaca fascicularis*). *J Physiol* 427: 681–713, 1990.

Shapley R, Perry VH. Cat and monkey retinal ganglion cells and their visual functional roles. *Trends Neurosci* 9: 229–235, 1986.

Sher A, DeVries SH. A non-canonical pathway for mammalian blue-green color vision. *Nat Neurosci* 15: 952–953, 2012.

Smith VC, Lee BB, Pokorny J, Martin PR, Valberg A. Responses of macaque ganglion cells to the relative phase of heterochromatically modulated lights. *J Physiol* 458: 191–221, 1992.

Smithson HE, Mollon JD. Is the S-opponent chromatic sub-system sluggish? *Vision Res* 44: 2919–2929, 2004.

Snowden RJ, Hess RF. Temporal frequency filters in the human peripheral visual field. *Vision Res* 32: 61–72, 1992.

Solomon SG, Lee BB, Sun H. Suppressive surrounds and contrast gain in magnocellular-pathway retinal ganglion cells of macaque. *J Neurosci* 26: 8715–8726, 2006.

Solomon SG, Lee BB, White AJ, Rüttiger L, Martin PR. Chromatic organization of ganglion cell receptive fields in the peripheral retina. *J Neurosci* 25: 4527–4539, 2005.

Solomon SG, Martin PR, White AJ, Rüttiger L, Lee BB. Modulation sensitivity of ganglion cells in peripheral retina of macaque. *Vision Res* 42: 2893–2898, 2002a.

Solomon SG, Tailby C, Cheong SK, Camp AJ. Linear and nonlinear contributions to the visual sensitivity of neurons in primate lateral geniculate nucleus. *J Neurophysiol* 104: 1884–1898, 2010.

Solomon SG, White AJ, Martin PR. Temporal contrast sensitivity in the lateral geniculate nucleus of a New World monkey, the marmoset *Callithrix jacchus*. *J Physiol* 517: 907–917, 1999.

Solomon SG, White AJ, Martin PR. Extraclassical receptive field properties of parvocellular, magnocellular and koniocellular cells in the primate lateral geniculate nucleus. *J Neurosci* 22: 338–349, 2002b.

Stockman A, Langendorfer M, Smithson HE, Sharpe LT. Human cone light adaptation: from behavioral measurements to molecular mechanisms. *J Vis* 6: 1194–1213, 2006.

Sun H, Smithson HE, Zaidi Q, Lee BB. Specificity of cone inputs to macaque retinal ganglion cells. *J Neurophysiol* 95: 837–849, 2006.

Swanson WH, Ueno T, Smith VC, Pokorny J. Temporal modulation sensitivity and pulse-detection thresholds for chromatic and luminance perturbations. *J Opt Soc Am A* 4: 1992–2005, 1987.

Szmajda BA, Buzás P, FitzGibbon T, Martin PR. Geniculocortical relay of blue-off signals in the primate visual system. *Proc Natl Acad Sci USA* 103: 19512–19517, 2006.

Tailby C, Solomon SG, Lennie P. Functional asymmetries in visual pathways carrying S-cone signals in macaque. *J Neurosci* 28: 4078–4087, 2008a.

Tailby C, Szmajda BA, Buzás P, Lee BB, Martin PR. Transmission of blue (S) cone signals through the primate lateral geniculate nucleus. *J Physiol* 586: 5947–5967, 2008b.

Tovée MJ, Bowmaker JK, Mollon JD. The relationship between cone pigments and behavioural sensitivity in a New World monkey (*Callithrix jacchus jacchus*). *Vision Res* 32: 867–878, 1992.

Tyler CW. Analysis of visual modulation sensitivity. II. Peripheral retina and the role of photoreceptor dimensions. *J Opt Soc Am A* 2: 393–398, 1985.

Vardi N, Duvoisin R, Wu G, Sterling P. Localization of mGluR6 to dendrites of ON bipolar cells in primate retina. *J Comp Neurol* 423: 402–412, 2000.

White AJ, Solomon SG, Martin PR. Spatial properties of koniocellular cells in the lateral geniculate nucleus of the marmoset *Callithrix jacchus*. *J Physiol* 533: 519–535, 2001.

Wiesel TN, Hubel D. Spatial and chromatic interactions in the lateral geniculate body of the rhesus monkey. *J Neurophysiol* 29: 1115–1156, 1966.

Williams PE, Mechler F, Gordon J, Shapley R, Hawken MJ. Entrainment to video displays in primary visual cortex of macaque and humans. *J Neurosci* 24: 8278–8288, 2004.

Yeh T, Lee BB, Kremers J. Temporal response of ganglion cells of the macaque retina to cone-specific modulation. *J Opt Soc Am A* 12: 456–464, 1995a.

Yeh T, Lee BB, Kremers J, Cowing JA, Hunt DM, Martin PR, Troy JB. Visual responses in the lateral geniculate nucleus of dichromatic and trichromatic marmosets (*Callithrix jacchus*). *J Neurosci* 15: 7892–7904, 1995b.

Zele AJ, Vingrys AJ. Cathode-ray-tube monitor artefacts in neurophysiology. *J Neurosci Methods* 141: 1–7, 2005.